

Quantum phase-slips in Josephson junction rings

G. Rastelli,^{1,2} I. M. Pop,^{3,4} and F.W.J. Hekking¹

¹*Université Grenoble 1/CNRS, LPMMC UMR 5493, B.P. 166, 38042 Grenoble, France*

²*Fachbereich Physik, Universität Konstanz, D-78457 Konstanz, Germany*

³*Institut Néel, CNRS, and Université Joseph Fourier, B.P. 166, 38042 Grenoble, France*

⁴*Department of Applied Physics, Yale University, New Haven, Connecticut 06520, USA*

(Dated: November 5, 2018)

We study quantum phase-slip (QPS) processes in a superconducting ring containing N Josephson junctions and threaded by an external static magnetic flux Φ_B . In a such system, a QPS consists of a quantum tunneling event connecting two distinct classical states of the phases with different persistent currents [K. A. Matveev et al., Phys. Rev. Lett. **89**, 096802 (2002)]. When the Josephson coupling energy E_J of the junctions is larger than the charging energy $E_C = e^2/2C$ where C is the junction capacitance, the quantum amplitude for the QPS process is exponentially small in the ratio E_J/E_C . At given magnetic flux each QPS can be described as the tunneling of the phase difference of a single junction of almost 2π , accompanied by a small harmonic displacement of the phase difference of the other $N - 1$ junctions. As a consequence, the total QPS amplitude ν_{ring} is a global property of the ring. Here we study the dependence of ν_{ring} on the ring size N , taking into account the effect of a finite capacitance C_0 to ground which leads to the appearance of low-frequency dispersive modes. Josephson and charging effects compete and lead to a non-monotonic dependence of the ring's critical current on N . For $N \rightarrow \infty$, the system converges either towards a superconducting or an insulating state, depending on the ratio between the charging energy $E_0 = e^2/2C_0$ and the Josephson coupling energy E_J .

PACS numbers: 74.50.+r, 74.81.Fa, 73.23.Ra, 85.25.Cp

I. INTRODUCTION

One-dimensional Josephson junction chains (1D JJ chains) have received considerable interest recently. Their use has been proposed for the realization of a qubit topologically protected against decoherence,¹⁻⁶ for the realization of a tunable parametric amplifier in narrow frequency ranges,^{7,8} for the realization of a fundamental current standard in quantum metrology,^{9,10} and for designing controlled inductive electromagnetic environments in quantum circuitry.^{11,12}

Homogeneous JJ chains of infinite length have been studied theoretically in the past.¹³⁻¹⁸ Such chains consist of superconducting islands, separated by Josephson tunnel junctions. In this paper we consider JJ chains arranged in a closed geometry, Fig. 1. The electrostatic interaction between the metallic islands is modeled by a neighboring capacitance C and by a local ground capacitance C_0 , with $E_C = e^2/2C$ and $E_0 = e^2/2C_0$ the corresponding charging energies. Each Josephson junction can sustain a maximum supercurrent $I_J = 2eE_J/\hbar$; this defines the Josephson coupling energy E_J .

Previous theoretical studies¹³⁻¹⁵ predicted a superconductor-insulator phase transition when the ratio between the Josephson energy E_J and the characteristic charging energy is reduced below a critical value. Bradley and Doniach studied this phase transition for infinite JJ chains and for the two extreme opposite cases when one of the two capacitances is vanishing ($C_0 = 0$ or $C = 0$).¹³ Korshunov investigated the general case for arbitrary ratio C/C_0 .^{14,15} He found that the critical value $E_J^{(c)}$ of the Josephson energy at which

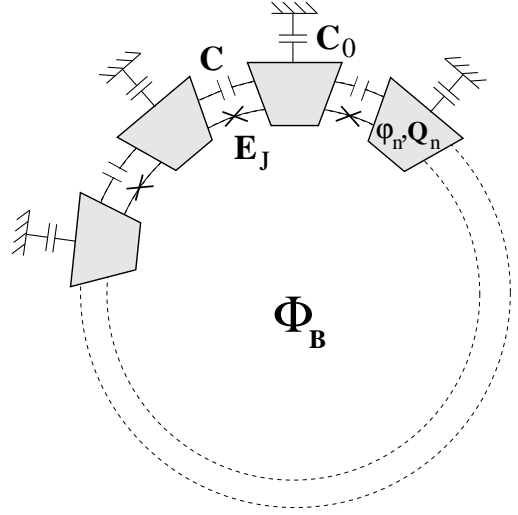


Figure 1: Schematic representation of a superconducting ring threaded by a magnetic flux Φ_B and containing N identical Josephson junctions with a mutual capacitance C and a local ground capacitance C_0 . E_J is the energy scale for the Josephson coupling. The variables (φ_n, Q_n) are, respectively, the condensate phase and the excess charge of the n th superconducting island.

the system undergoes the phase transition equals to $E_J^{(c)} = E_0 f(C/C_0)$ where $f(x)$ is a smooth and regular function of order one. In particular, for the case $C_0 = 0$, we have $E_0 = \infty = E_J^{(c)}$ and the system is an insulator for *any value of E_J* in agreement with the result of Bradley and Doniach.¹³ Subsequently, experimental

studies of the finite temperature behavior of the residual resistance in long one-dimensional chains of SQUIDS reported a phase transition when reducing the Josephson energy.^{19–23}

The theoretical results reviewed so far were obtained in the thermodynamic limit $N \rightarrow \infty$. A first attempt to go beyond this limit was undertaken by Matveev, Glazman and Larkin²⁴ who studied quantum phase-slip (QPS) processes in a superconducting nanoring containing a large, but finite number of Josephson junctions. Here a QPS consists of a quantum tunneling between two distinct classical states of the phases with different persistent currents circulating in the ring at given magnetic flux.²⁴ This is a collective process which can be described as the tunneling of the phase difference of a single junction by *almost* 2π , accompanied by a small harmonic displacement of the phase difference of the other $N - 1$ junctions (see Ref. 24 and the explanation in Sec. III B). Quantum tunneling is possible due to the finite junction capacitance, which plays the role of inertia.

Matveev et al. predicted a strong reduction of the maximum critical current sustained by the ring with increasing ring size N due to QPS processes. Recent experiments on flux-biased rings containing a few Josephson junctions²⁵ indeed reported a remarkable suppression of the maximum supercurrent as E_J/E_C decreases, in agreement with the findings of Ref. 24. In these devices, the effects of the capacitance to ground could be neglected since the ring's circumference was much smaller than the screening length λ of the system, given by $\lambda = \pi\sqrt{C/C_0}$. However, it is expected that, for JJ rings of intermediate circumference $N \gtrsim \lambda$, the effects of the capacitance to ground can no longer be ignored.

In this paper, we study a JJ ring of finite circumference and threaded by an external magnetic flux Φ_B , Fig. 1. Specifically, we consider properties of the flux-dependent thermodynamic persistent current. We go beyond the previous work of Matveev et al.²⁴ and we take into account the collective nature of a QPS as well as the ground capacitance C_0 for calculating the QPS amplitude. We show that the interplay between the finite value of the ratio C_0/C and finite size effects gives rise to a non-monotonic dependence of the low-energy properties on N . We systematically discuss this interplay as well as its consequences for the QPS amplitude for flux-biased rings with arbitrary number $N \gtrsim 5$. For shorter lengths, a detailed numerical analysis was realized in 26.

We focus on the limit where the Josephson coupling energy E_J dominates over the charging energies E_C, E_0 , such that the amplitude for QPS to occur is exponentially small in the ratio E_J/E_C . This fact allows us to focus on the analysis of a single QPS event. Once the QPS amplitude is known, one can calculate the ring's low-energy spectrum as a function of the external flux Φ_B and hence obtain the maximum supercurrent I_{\max} that the ring can sustain.

II. QUALITATIVE DISCUSSION AND MAIN RESULTS

Our main results are summarized in Fig. 2, where we show the dependence of I_{\max} – scaled to the classical value $I_{\text{cl}} = \pi I_J/N$ found in the absence of QPS processes – as a function of N for two relevant situations: $C_0 = 0$ and $C_0 = C/2$.

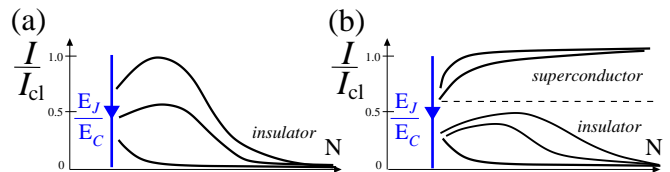


Figure 2: Schematic behavior of the maximum supercurrent I_{\max} in 1D JJ rings as a function of N , scaled to the classical value I_{cl} , for different values of the ratio E_J/E_C for (a) $C_0 = 0$ and (b) $C_0 = C/2$ (see also Fig. 8 and Fig. 11 for details).

As we will discuss in detail below, a QPS can be described as a $2\pi(1 - 1/N)$ winding of the local phase-difference occurring on one of the junctions, accompanied by a simultaneous small (harmonic) adjustment of the phases of the other $N - 1$ junctions.²⁴ In a first approximation, the winding of the phase on one of the junctions can be characterized by the amplitude for the quantum tunneling between two different minima of the Josephson potential. It is given by^{24,27–29}

$$\nu_0 = \frac{4}{\sqrt{\pi}} (8E_J^3 E_C)^{\frac{1}{4}} \exp\left(-\sqrt{8\frac{E_J}{E_C}}\right). \quad (1)$$

The dynamics of the simultaneous small adjustment depends crucially on the capacitance ratio C_0/C .

Consider first the case $C_0 = 0$, Fig. 2(a). The other $N - 1$ junctions form a bath of dispersionless harmonic oscillators, all having the same (plasma) frequency $\omega_p = (8E_J E_C)^{1/2}/\hbar$. In order to satisfy the constraint imposed by the flux threading the ring at all times during the QPS process, the phase differences for the $N - 1$ other junctions perform a small shift $\sim 1/N$. This adjustment gives rise to finite-size corrections for intermediate ring circumferences N to the amplitude given by Eq. (1) leading to a QPS amplitude $\nu_0 \rightarrow \nu(N)$. Since any junction can act as a QPS center, the total QPS amplitude for the ring is given by $\nu_{\text{ring}} = N\nu(N)$.

In the limit $N \gg 1$, finite size effects vanish and $\nu(N)$ converges to the constant ν_0 so that ν_{ring} increases with the length and the maximum supercurrent I_{\max} vanishes exponentially,²⁴ see Fig. 2(a). The system becomes a perfect insulator at $N = \infty$, in agreement with Refs. 13–15. On the other hand, we find that the interplay between charging and Josephson effects in finite systems leads to an *enhancement* of the effective QPS amplitude $\nu(N)$ with *decreasing* ring circumference N , $\nu(N) \sim \nu_0 \exp[(E_J/E_C)^{1/2}/N]$, thus reducing the maximum supercurrent I_{\max} . Consequently, the maximum

supercurrent I_{\max} shows non-monotonic behavior as a function of the ring circumference N for sufficiently large values of the ratio E_J/E_C .

When the capacitance to ground C_0 is restored, the $N-1$ harmonic junctions interact directly between them. This leads to the appearance of an ensemble of $N-1$ dispersive electrodynamic modes at frequencies below ω_p , similar to the ones found in a standard LC-transmission line.³⁰ The tunneling phase couples to these modes in much the same way as a quantum particle to a harmonic bath in the Caldeira-Leggett model.³¹ In particular, the low-frequency modes with linear dispersion $\hbar\omega_k \sim (8E_J E_0)^{1/2} \pi k/N$ give rise to a finite friction for the QPS dynamics in the limit $N = \infty$.

At finite N , the coupling with the low-frequency modes strongly affects the QPS amplitude. Indeed, we find that $\nu(N) \sim \nu_0/N^\alpha$ for $N \gg 1$ where $\alpha \propto (E_J/E_0)^{1/2}$. Depending on the value of α , $\nu_{\text{ring}} = N\nu(N) \sim N^{1-\alpha}$ either tends to zero, when $\alpha \gg 1$, or grows linearly, when $\alpha \ll 1$, indicating that the system either displays a superconducting or an insulating behavior, as can be seen in Fig. 2(b). This behavior is reminiscent of the dissipative phase transition³² occurring in a single junction in an electromagnetic environment.^{14,15} For intermediate ring sizes, finite size effects occur, yielding a non-monotonic behavior of the maximum supercurrent in the insulating regime, similar to what we find for the case $C_0 = 0$.

The paper is structured as follows. In Sec. III we recall the model for a flux-biased 1D JJ ring as well as the notion of QPS and the approximations involved to find the ring's flux-dependent quantum ground state and hence the maximum supercurrent. In Sec. IV we discuss the single QPS approximation and we show how the system reduces to a model similar to that of Caldeira and Leggett³¹ where one single Josephson junction, the center of the QPS, is coupled to $N-1$ harmonic oscillators. The results for the specific case $C_0 = 0$ are shown in Sec. V where we explain in detail the different finite-size corrections on the QPS amplitude. The effect of the finite ground capacitance $C_0 > 0$ and the general results are discussed in Sec. VI. In the last Section VII we draw our conclusions.

III. THE MODEL

A. Hamiltonian

We consider a homogeneous ring of N identical superconducting islands each coupled to its nearest neighbor by Josephson tunnel junctions, see Fig. 1. The ring is threaded by a magnetic flux Φ_B . We assume the superconducting gap Δ of the islands to be the largest energy scale involved in the problem. If $\Delta \gg \delta E$ where δE is the average spacing of the electronic energy levels, superconductivity is well established. The islands should be metallic with large enough volume so that the perturbative treatment of Cooper pair tunneling through

the contacting surfaces is justified. We assume the absence of quasi-particle excitations at low temperature T and low voltage $k_B T, 2e\bar{V} \ll \Delta$, where \bar{V} is the typical voltage across the junctions. Furthermore, the condition $\Delta \gg E_C, E_0$ implies that the Josephson coupling energy E_J characterizing Cooper-pair-tunneling between islands is independent of E_C, E_0 .

We assume that the kinetic inductance, associated with the kinetic energy of the Cooper pairs in each superconducting island, is negligible as compared to the Josephson inductance.^{33,34} We also assume that the geometric inductance can be neglected so that the current circulating in the ring does not generate any magnetic field. The total flux Φ_B is thus only given by the externally applied magnetic field.

The previous conditions define the standard quantum-phase model for a 1D-JJ homogeneous chain whose Hamiltonian reads¹⁶

$$H = \frac{1}{2} \sum_{n,m=0}^{N-1} \hat{Q}_n \bar{C}_{nm}^{-1} \hat{Q}_m - E_J \sum_{n=0}^{N-1} \cos \left(\hat{\varphi}_{n+1} - \hat{\varphi}_n + \frac{2\pi\Phi_B}{N\Phi_0} \right), \quad (2)$$

where Φ_0 is the flux quantum. For each island, the BCS condensate phase $\hat{\varphi}_n$ and the excess charge \hat{Q}_n on the n th island represent the conjugate variables of the system $[\hat{\varphi}_n, \hat{Q}_n] = 2ei$. \bar{C} is the capacitance matrix with matrix elements $\bar{C}_{n,m} = (C_0 + 2C)\delta_{n,m} - C(\delta_{n+1,m} + \delta_{n-1,m})$, with the index $n = -1$ corresponding to $N-1$ and $n = 0$ corresponding to N . The relative phase-difference across the n th junction is $\hat{\theta}_n = \hat{\varphi}_{n+1} - \hat{\varphi}_n$. As the phases are compact variables, *i.e.* $\hat{\varphi}_N = \hat{\varphi}_0 + 2\pi m$ where m is an integer, we have the constraint on the phase-differences for Josephson junctions in a ring³⁵

$$\sum_{n=0}^{N-1} \hat{\theta}_n = 2\pi m. \quad (3)$$

Note that the argument of each cosine in Eq. (2) is the gauge-invariant phase-difference across the corresponding junction.

From Eqs. (2) and (3) we see that the physical properties of the system depend periodically on the ratio $\delta = 2\pi\Phi_B/\Phi_0$. In the steady-state regime, the dc-supercurrent flowing through the ring is the same for all the junctions $\langle \hat{I}_n \rangle = I$ and can be related to the derivative of the ground state energy E_{GS} of the system with respect to δ

$$I(\delta) = \frac{\partial E_{GS}}{\partial \Phi_B} = \left(\frac{2e}{\hbar} \right) \frac{\partial E_{GS}}{\partial \delta}. \quad (4)$$

It is in general a difficult task to find the ground-state energy $E_{GS}(\delta)$ for the flux-biased ring described by Hamiltonian (2) and (3). An approximate solution can be found in the limit where the Josephson energy is larger than the characteristic electrostatic energy $E_J \gg E_C, E_0$, which is the regime discussed in this paper.

B. Single QPS in JJ rings of finite circumference

To set the stage, let us first consider the classical limit, achieved by setting $E_C = E_0 = 0$, so that the phases are well-defined classical variables. The classical energy of the system reduces to

$$E_{cl} = -E_J \sum_{n=0}^{N-1} \cos\left(\theta_n + \frac{\delta}{N}\right). \quad (5)$$

The energy Eq. (5) is invariant under a change by 2π of the phases θ_n . In other words, the states θ_n and $\theta_n + 2\pi k$ are equivalent (k integer). However, at fixed magnetic flux δ , a given configuration of $\{\theta_n\}$ corresponds to a real physical state *only if* the constraint Eq. (3) is satisfied. Therefore any distribution of the phases that violates Eq. (3) is unphysical.

The classical states $|m\rangle$ that minimize the energy Eq. (5) under the constraint (3) correspond to a uniform distribution of phase differences $\theta_n = 2\pi m/N$. They have energies

$$E_m = -E_J N \cos\left(\frac{2\pi m + \delta}{N}\right), \quad (6)$$

with the condition $d^2 E_{cl}/d\theta_n^2|_m = -E_m > 0$ and the index $-(N-1)/2 < m < (N-1)/2$ (N odd) or $-N/2 < m < (N/2) - 1$ (N even). These classical states $|m\rangle$ are physically *distinguishable* as they are characterized by different persistent currents

$$I_m = I_J \sin\left(\frac{2\pi m + \delta}{N}\right). \quad (7)$$

Away from the degeneracy points $\delta = 0$ and $\delta = \pi$ they also have different energies. The classical ground state corresponds to an absolute minimum

$$E_{GS}^{(cl)} = -E_J N \max_m \cos\left(\frac{2\pi m + \delta}{N}\right) \simeq \frac{E_J}{2N} \min_m (2\pi m + \delta)^2, \quad (8)$$

where the second, approximate equality is numerically accurate for sufficiently long rings ($N \gtrsim 5$). The corresponding supercurrent then has a sawtooth-like dependence as a function of δ with a maximum supercurrent given by $I_{cl} \simeq \pi I_J/N$.²⁴

For finite C, C_0 , the electrostatic interaction acts as an inertial term on the phases so that quantum fluctuations occur, giving rise to quantum phase-slips (QPSs). At fixed magnetic flux and in a ring of finite circumference, the QPS is a collective process corresponding to the *quantum tunneling in a multidimensional space* of dimension N between two distinct minima of the potential, corresponding for instance to the classical states $|m\rangle$ and $|m+1\rangle$, separated by some energy barrier associated with the potential Eq. (5). In the multidimensional space, the physical paths $\{\theta_n\}$ which connect $|m\rangle$ and $|m \pm 1\rangle$ correspond to a subspace defined by the constraint Eq. (3). Due to this constraint, the multidimensional tunneling reduces to one-dimensional tunneling in

which we have only a few trajectories connecting the initial state and the final state, see Fig. 3. As it was discussed in Ref. 24, an example of QPS connecting the states $|m\rangle$ and $|m+1\rangle$ is given by the displacements

$$\theta_{n_0} = \frac{2\pi m}{N} \longrightarrow \frac{2\pi(m+1)}{N} - 2\pi, \quad (9)$$

$$\theta_n = \frac{2\pi m}{N} \longrightarrow \frac{2\pi(m+1)}{N} \quad (n \neq n_0), \quad (10)$$

in which the local phase difference θ_{n_0} , n_0 being the center of the QPS, winds by an amount of $2\pi(1 + 1/N)$ and the whole set of phase differences $\{\theta_n\}$ ($n \neq n_0$) shifts in order to preserve the constraint. Fig. 3a shows this process. One can express the classical energy Eq. (5) as $E_{cl}/E_J = -\cos(\theta_{n_0} + \delta/N) - (N-1)\cos(\theta_n + \delta/N)$ with $n \neq n_0$, Fig. 3b.

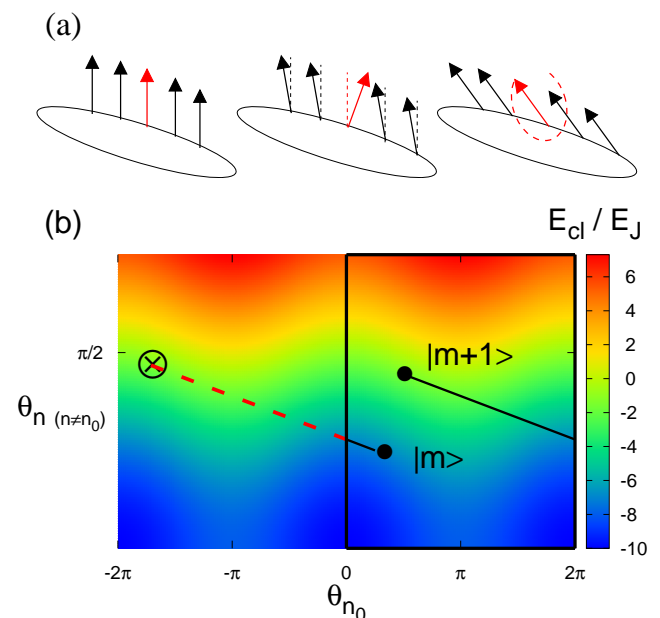


Figure 3: Example of a QPS process. **a)** The oval loop represents the JJ ring. The arrows represent a few phase differences $\{\theta_n\}$ around the QPS center at n_0 , the phase θ_{n_0} winding of $2\pi(1 - 1/N)$ (red arrow). The initial configuration (left) is the state $|m\rangle$ and the final configuration (right) is $|m+1\rangle$. The central configuration is intermediate between the two states $|m\rangle$ and $|m+1\rangle$. **b)** The classical energy expressed as $E_{cl}/E_J = -\cos(x) - (N-1)\cos(y)$ with the axis $x = \theta_{n_0} - \delta/N$ and $y = \theta_n - \delta/N$ ($n \neq n_0$). The dots represent the state $|m\rangle$ and $|m+1\rangle$. The cross also represents the state $|m+1\rangle$ but in the extended zone scheme. The black lines represent the physical trajectory of the QPS that connects the initial and the final state, the (black) solid one in the restricted zone scheme, the (red) dashed line in the extended zone scheme. The bold line for the borders marks the compact region. Parameters: $N = 10, \delta = \pi/2, m = 1$.

As it is shown in Fig. 3b, the trajectory of the QPS Eqs. (9),(10) can be drawn in a restricted, compact zone scheme as well as in an extended one. This fact allows

us to introduce the adiabatic potential for the QPS process. In the limit in which the evolution of the phases is extremely slow, the kinetic energy can be neglected at any time and one obtains the energy of the system just minimizing the classical energy for each intermediate configuration which connects the initial and the final state. Hence the adiabatic potential is associated with the line of minimum energy on the surface Eq. (5) which connects the end points as shown in the example of Fig. 3b. This line is given by the condition

$$\theta_n = \frac{2\pi m - \theta_{n_0}}{N-1} \quad (n \neq n_0). \quad (11)$$

After a shift of the phase $\theta_{n_0} \rightarrow \theta_{n_0} - \delta/N$, the effective adiabatic potential $V_{eff}(\theta_{n_0})$ reads

$$\begin{aligned} V_{eff}(\theta_{n_0}) &= -E_J \left[\cos(\theta_{n_0}) + (N-1) \cos\left(\frac{\delta + 2\pi m - \theta_{n_0}}{N-1}\right) \right] \\ &\simeq E_J \left[-\cos(\theta_{n_0}) + \frac{(\delta + 2\pi m - \theta_{n_0})^2}{2(N-1)} \right], \quad (12) \end{aligned}$$

where the second, approximate equality is valid for sufficiently long rings ($N \gtrsim 5$). At the initial time we have $V_{eff}[\theta_{n_0} = (\delta + 2\pi m)/N] = E_m$ and at the final time $V_{eff}[\theta_{n_0} = 2\pi + [\delta + 2\pi(m+1)]/N] = E_{m+1}$. In Fig. 4, we show $V_{eff}(\theta_{n_0})$.

In the limit of $N \rightarrow \infty$ we have $V_{eff}(\theta_{n_0}) = -E_J \cos(\theta_{n_0})$ and we recover the simplified picture of QPS corresponding to the quantum tunneling of the phase difference θ_{n_0} of a given junction n_0 from one minimum of the local Josephson potential $-\cos(\theta_{n_0})$ to the neighboring one.

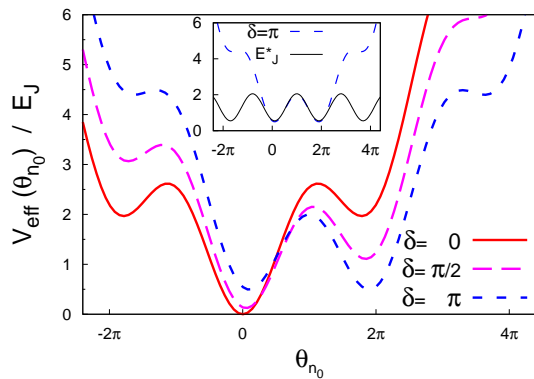


Figure 4: Example of the effective potential $V_{eff}(\theta_{n_0})$ Eq. (12) for $N = 10$ and for the values $\delta = 0$ solid (red) line, $\delta = \pi/2$ dashed (purple) line and $\delta = \pi$ dotted (blue) line. Inset: comparison between the effective potential at $\delta = \pi$, dotted (blue) line, with the cosine potential $E_J^* \cos[\theta_{n_0}(N-1)/N]$, solid line (see text).

On the other hand, as we explained above, QPS is a collective process corresponding to a quantum tunneling in a multidimensional space with the constraint Eq. (3). Consequently, the potential in terms of the variable θ_{n_0} ,

the center of the QPS, is *not a periodic* function although the global classical energy of the system Eq. (5) is 2π periodically invariant.

C. Effective low-energy description

We now turn to the effects of quantum phase fluctuations in the limit $E_J \gg E_C, E_0$. In this case, a simple analysis is possible since the QPS processes occur only rarely, with an exponentially small amplitude ν , Eq. (1). The single QPS approximation is further analyzed in Sec. VID and Sec. VIE, where we estimate its range of validity.

As a consequence of QPSs and for small amplitude ν , the quantum ground state $|\Psi_{GS}\rangle$ of the ring corresponds to a superposition of different classical states of the phases, namely $|\Psi_{GS}\rangle = \sum_m c_m |m\rangle$. The coefficients c_m as well as the quantum ground state energy $E_{GS}(\delta)$ can be obtained from the following effective Schrödinger equation²⁴

$$E_m c_m - \nu_{\text{ring}} (c_{m+1} + c_{m-1}) = E_{GS} c_m, \quad (13)$$

where the term proportional to $\nu_{\text{ring}} \equiv N\nu$ connects two classical states differing by a single QPS. The factor N takes into account the fact a QPS can have the center in any junction of the chain and this corresponds to different trajectories in the multidimensional space N so that QPS amplitudes add up coherently. This coherence has been recently confirmed experimentally in a short 6-SQUID JJ chain³⁶ by the measurements of the Aharonov-Casher interference effect. The coherence is affected by off-set charge dynamics. The details of this dynamics are currently not understood. It is expected to give rise to an additional dependence of ν on N which is beyond the scope of the present paper.

The behavior of the general solution for the ground-state of the model given by Eq. (13) is determined by only one dimensionless parameter

$$q = \frac{N^2 \nu(N)}{2\pi^2 E_J}. \quad (14)$$

The ground-state energy $E_{GS} = E_{GS}(\delta; q)$ depends parametrically on q , hence leading to a dependence of the maximum supercurrent $I_{\text{max}}(q)$ on the QPS amplitude ν . This dependence is illustrated in Fig. 5 together with the evolution of the value of the phase δ_{max} that corresponds to the maximum. For $q \ll 1$, the solution scales as $I_{\text{max}}/I_{\text{cl}} \simeq 1 - (5/2)q^{2/3}$ whereas it scales as $I_{\text{max}}/I_{\text{cl}} \simeq 24\sqrt{\pi}q^{4/3} \exp(-8\sqrt{q})$ for $q \gg 1$.

The effective low-energy theory defined by (13) was introduced in Ref. 24 for $C_0 = 0$ and was discussed for long JJ rings $N \gg 1$. As we discussed in sec. IIIB, the validity of Eq. (13) extends more generally to include rings of intermediate size and with $C_0 \neq 0$. In the following, we will obtain the detailed dependence of the QPS amplitude ν_{ring} on the parameters N , E_J , E_C , and E_0 . Hence,

we calculate the ground state energy of the system using Eq. (13) to obtain the periodic dependence of $E_{GS}(\delta)$ and $I(\delta)$ on δ , Eq. (4), from which we extract I_{max} .

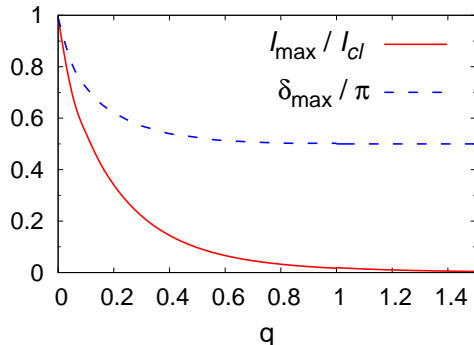


Figure 5: Maximum supercurrent (solid line) for the model defined by Eq. (13) as a function of q , Eq. (14). The dashed line represents the value of the scaled flux δ_{max} which gives the maximum supercurrent.

IV. QPS IN 1D JJ RING

A. General approach for a single QPS event

We present a general approach to calculate the quantum amplitude ν for a single QPS event occurring on a ring containing N junctions and with mutual and ground capacitance C and C_0 , in the regime $E_J \gg E_C, E_0$.

According to Eqs. (9) and (10), the QPS process is a collective process in which the local phase difference θ_{n_0} winds by an amount of $2\pi(1 - 1/N)$, accompanied by a shift of the whole set of phase differences $\{\theta_n\}$ ($n \neq n_0$). For rings of circumference $N \gtrsim 5$, the phase differences of the other junctions will vary only slightly $\Delta\theta_n \sim 1/N$ compared to the period 2π of the cosine potential. Hence we can apply the harmonic approximation to describe the dynamics corresponding of θ_n , $n \neq n_0$.

For vanishing ground capacitance $C_0 = 0$, the phase-differences of the other $N - 1$ junctions behave as independent LC -oscillators at the plasma frequency ω_p whose displacement is inversely proportional to the circumference N . Thus, in the limit of a very large ring $N \gg 1$, the dynamics of the other $N - 1$ phase differences can be neglected²⁴ so that the QPS amplitude $\nu(N)$ can be approximated by the N -independent constant value ν_0 , Eq. (1). However, for 1D-JJ rings of finite circumference, the dynamics of the other junctions can have considerable effects on ν , as we will show below. Moreover, for finite ground capacitance $C_0 > 0$ the harmonic oscillations of the phase-differences of the $N - 1$ junctions play a crucial role for any ring's circumference.

To calculate the QPS amplitude ν , we start by considering the partition function associated with the Hamiltonian Eq. (2), with the constraint Eq. (3). In the path

integral formalism, it reads ($\beta = \hbar/k_B T$)

$$\mathcal{Z} = \text{Tr} \left[e^{-\frac{\beta}{\hbar} \hat{H}} \right] = \prod_{n=0}^{N-1} \oint \mathcal{D}[\varphi_n(\tau)] e^{-S/\hbar}, \quad (15)$$

where the Euclidean action for the phases $\{\varphi_n(\tau)\}$ reads $S = \int_0^\beta d\tau \mathcal{L}$, and \mathcal{L} is the Lagrangian,

$$\begin{aligned} \mathcal{L} = & \sum_{n=0}^{N-1} \frac{\hbar^2 C_0}{8e^2} \dot{\varphi}_n^2 + \sum_{n=0}^{N-1} \frac{\hbar^2 C}{8e^2} (\dot{\varphi}_{n+1} - \dot{\varphi}_n)^2 \\ & - \sum_{n=0}^{N-1} E_J \cos \left(\varphi_{n+1} - \varphi_n + \frac{\delta_m}{N} \right), \end{aligned} \quad (16)$$

with $\dot{\varphi}_n = d\varphi/d\tau$ and $\delta_m = \delta + 2\pi m$. The compact variables $\{\varphi_n\}$ are defined on the circle $[0; 2\pi[$. Notice that we shifted the phase differences $\{\theta_n\}$ with respect to their average value so that Eq. (3) now reads $\sum_{n=0}^{N-1} \theta_n = 0$. The last constraint is automatically satisfied by imposing the boundary condition $\varphi_N = \varphi_0$.

B. Harmonic modes

Let us briefly discuss the behavior of the system in the harmonic approximation, neglecting the QPS. When the Josephson energy $E_J \gg E_C, E_0$ the phases fluctuate only slightly around their classical values. The average phase difference between the neighboring islands is small so that we can expand the Josephson interaction to lowest (quadratic) order. The general imaginary-time Lagrangian Eq. (16) then reduces to the harmonic one,

$$\begin{aligned} \mathcal{L}_{har}^{(N)} = & \sum_{n=0}^{N-1} \frac{\hbar^2 C_0}{8e^2} \dot{\varphi}_n^2 + \sum_{n=0}^{N-1} \frac{\hbar^2 C}{8e^2} (\dot{\varphi}_{n+1} - \dot{\varphi}_n)^2 \\ & + \sum_{n=0}^{N-1} \frac{1}{2} E_J (\varphi_{n+1} - \varphi_n)^2 + \frac{E_J}{2N} \delta_m^2, \end{aligned} \quad (17)$$

where we omitted an irrelevant constant term. Any periodic function φ_n defined on the finite lattice $n = 0, \dots, N - 1$ can be decomposed as

$$\varphi_n = \frac{1}{\sqrt{N}} \sum_{k=0}^{N-1} \varphi_k e^{i \frac{2\pi}{N} kn}, \quad (18)$$

with the condition for the complex variables $\varphi_{N-k} = \varphi_k^*$ which preserves the total number of degrees of freedom. Substituting Eq. (18) into Eq. (17) and summing over the index n , the harmonic Lagrangian is diagonalized (see also Appendix A)

$$\mathcal{L}_{har}^{(N)} = \sum_{k=0}^{N-1} \left(\frac{1}{2} \mu_k |\dot{\varphi}_k|^2 + \frac{1}{2} \mu_k \omega_k^2 |\varphi_k|^2 \right) + \frac{E_J}{2N} \delta_m^2. \quad (19)$$

We have introduced the constants

$$\mu_k = \frac{\hbar^2}{4e^2} \left\{ C_0 + 2C \left[1 - \cos \left(\frac{2\pi}{N} k \right) \right] \right\}; \quad (20)$$

the frequency dispersion is given by

$$\omega_k = \omega_p \sqrt{\frac{1 - \cos\left(\frac{2\pi k}{N}\right)}{1 - \cos\left(\frac{2\pi k}{N}\right) + \frac{\pi^2}{2\lambda^2}}}, \quad (21)$$

where the screening length is $\lambda = \pi\sqrt{C/C_0}$. For $N \gg 1$, the maximal frequency of the modes ω_{max} is given by

$$\omega_{max} = 4\sqrt{\frac{E_J}{\hbar^2} \left(\frac{e^2}{4C + C_0}\right)}. \quad (22)$$

An example of this frequency dispersion is given in Fig. 6. We can distinguish two regimes for $C_0 > 0$. For JJ rings longer than the screening length λ , $N \gg \lambda$, the spectrum has a linear dispersion for low frequencies. For shorter rings $N \ll \lambda$, the lowest mode appears almost at the plasma frequency ω_p and the linear behavior is completely absent. For the case $C_0 = 0$ we recover a flat distribution where all the modes are degenerate and correspond to the plasma frequency ω_p .

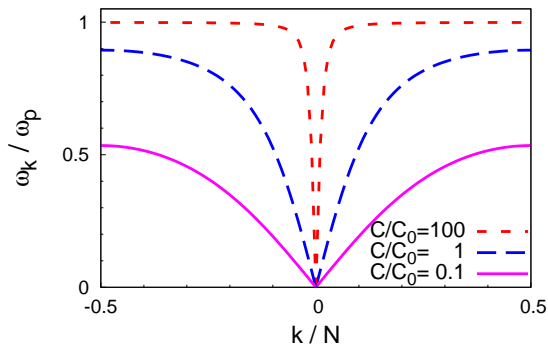


Figure 6: Frequency dispersion of the harmonic modes in a JJ ring of $N = 100$ junctions. We use the equivalent index notation $k = -N/2 + 1, \dots, N/2$. Solid (purple) line, dashed (blue) line and dotted (red) line are, respectively, for the ratio $C/C_0 = 0.1, 1, 100$.

Let us calculate the phase-dependent ground state energy $E_{GS}^{(har)}(\delta)$ in the harmonic approximation. The path integral in Eq. (15) can be explicitly calculated for the diagonalized harmonic action Eq. (19). We obtain

$$\mathcal{Z}_{har}^{(N)} \sim \left(\prod_{k \neq 0} \frac{1}{2 \sinh(\beta \omega_k / 2)} \right) e^{-\frac{\beta E_J}{2\hbar N} \min_m \delta_m^2}, \quad (23)$$

where the product corresponds to the partition function for an ensemble of $N-1$ independent harmonic oscillators and the exponential factor contains the classical energy of the system (mod 2π) at finite temperature. Notice that the zero frequency mode $k = 0$ is not involved in the relevant part of the partition function. Note also the periodicity of the result Eq. (23) with respect to δ . The quadratic dependence on δ in each of the segment $-\pi + 2\pi m < \delta < -\pi + 2\pi(m+1)$ is a consequence of the harmonic approximation, *i.e.*, Eq. (8).

We thus obtain the phase-dependent ground-state energy, $E_{GS}^{(har)} = -\lim_{\beta \rightarrow \infty} (\hbar/\beta) \ln \mathcal{Z}_{har}^{(N)}$

$$E_{GS}^{(har)} = \sum_{k \neq 0} \frac{\hbar \omega_k}{2} + \frac{E_J}{2N} \min_m \delta_m^2. \quad (24)$$

Notice that to reach the full quantum regime of the harmonic modes, as expressed by Eq. (24), the temperature has to be much smaller than the energy of the lowest mode, $k_B T \ll \hbar \omega_{min}$, which is given by

$$\omega_{min} = \omega_{max} \frac{\pi}{N} \sqrt{\frac{1 + \left(\frac{2\lambda}{\pi}\right)^2}{1 + \left(\frac{2\lambda}{N}\right)^2}}. \quad (25)$$

We conclude that, in the absence of QPS processes, the JJ ring forms a closed quantum *LC*-line (each Josephson junction in Fig. 1 is replaced by an inductance $L_J = \hbar^2/4e^2 E_J$) formed by $N-1$ independent harmonic oscillators with eigenfrequencies ω_k . The classical sawtooth relation between the supercurrent and the total phase $I = I(\delta)$ is unmodified by the quantum harmonic fluctuations of the phases. However, harmonic fluctuations are relevant when the QPSs are restored, as we will now show.

C. Effective QPS action in the presence of harmonic modes

We now turn our attention to the effect of the harmonic modes on the QPS amplitude. We will restrict our analysis to the limit in which the frequency of the lowest mode ω_{min} is greater than the frequency ν/\hbar associated to the tunneling in the effective (static) potential V_{eff} Eq. (12). In this adiabatic limit, the problem can be reduced to an effective two-state problem involving tunneling between neighboring states m and $m+1$ (see also Sec. VI E).

As discussed in Sec. III B, when a single QPS is centered on one specific junction n_0 , the dynamics of the other junctions ($n \neq n_0$) is well described by the harmonic approximation. Then, as seen in Sec. IV B, we can consider this part of the ring as an electromagnetic environment formed by $N-1$ independent harmonic oscillators and to which the single junction, center of the QPS process, is coupled. Accordingly, it is natural to cast the full action in a form where the winding phase-difference θ_{n_0} is linearly coupled to an ensemble of harmonic oscillators acting as an external bath.

Without loss of generality, one can assume the center of the QPS to the junction $n_0 = N-1$, namely $\theta = \theta_{N-1} = \varphi_0 - \varphi_{N-1}$. It is useful to introduce the average value of the phase at the junction $N-1$, namely $\Theta_0 = (\varphi_0 + \varphi_{N-1})/2$, so that one can write

$$\varphi_0 = \Theta_0 + \frac{\theta}{2}, \quad \varphi_{N-1} = \Theta_0 - \frac{\theta}{2}. \quad (26)$$

We choose as the relevant variables the set S given by the winding phase difference θ together with the local phases φ_n with $n = 1, \dots, N-2$.

First we discuss the harmonic expansion of the potential energy of the Lagrangian Eq. (16). In a QPS, the phase-differences across the junctions remain small with respect to 2π except at the junction $n_0 = N - 1$,

$$\sum_{n=0}^{N-1} \cos\left(\theta_n + \frac{\delta_m}{N}\right) \simeq \cos\left(\theta + \frac{\delta_m}{N}\right) - \frac{1}{2} \sum_{n=0}^{N-2} \left(\theta_n + \frac{\delta_m}{N}\right)^2. \quad (27)$$

Using the set S , the last sum in Eq. (27) contains a quadratic coupling between θ and the quantities $\Theta_0 - \varphi_1$ and $\Theta_0 - \varphi_{N-2}$. Although these terms contain θ varying by almost 2π , this does not make invalid our expansion as the overall argument of the cosine function, representing the phase-difference in the neighboring junctions $n = 0$ and $n = N - 2$, remains small during the QPS.

Using the set S , the Lagrangian of Eq. (16) is decomposed as

$$\mathcal{L} = \mathcal{L}_1 + \mathcal{L}_2 + \mathcal{L}_3, \quad (28)$$

where the first term \mathcal{L}_1 is associated with the winding junction

$$\mathcal{L}_1 = \frac{\hbar^2(3C + C_0)}{16e^2} \dot{\theta}^2 - E_J \cos\left(\theta + \frac{\delta_m}{N}\right) + E_J \left(\frac{\theta^2}{4} - \theta \frac{\delta_m}{N}\right). \quad (29)$$

The second term \mathcal{L}_2 describes the environment to which θ is coupled. Hereafter we change the notation for the average

$$\Theta_0 \rightarrow \varphi_0, \quad (30)$$

in order to simplify the following formulas. Then \mathcal{L}_2 reads

$$\begin{aligned} \mathcal{L}_2 = & \frac{\hbar^2 C_0}{8e^2} \dot{\varphi}_0^2 + \sum_{n=0}^{N-2} \frac{\hbar^2}{8e^2} \left[C_0 \dot{\varphi}_n^2 + C(\dot{\varphi}_{n+1} - \dot{\varphi}_n)^2 \right] \\ & + \sum_{n=0}^{N-2} \frac{1}{2} E_J (\varphi_{n+1} - \varphi_n)^2 + E_J (N-1) \left(\frac{\delta_m}{N}\right)^2, \end{aligned} \quad (31)$$

with the periodic boundary condition, $n = 0$ corresponding to $n = N - 1$. Note the extra term in Eq. (31) associated with the (average) phase at $n = 0$. The last term \mathcal{L}_3 of Eq. (28) describes the coupling between the winding junction and the electromagnetic environment,

$$\mathcal{L}_3 = \frac{\hbar^2 C}{8e^2} (\dot{\varphi}_{N-2} - \dot{\varphi}_1) \dot{\theta} + \frac{E_J}{2} (\varphi_{N-2} - \varphi_1) \theta. \quad (32)$$

We rewrite the Lagrangians \mathcal{L}_2 and \mathcal{L}_3 in terms of the normal modes φ_k . They are given by Eq. (18) with N replaced by $N - 1$. In terms of these modes, we have

$$\mathcal{L}_2 = \frac{\hbar^2 C_0}{8e^2} \dot{\varphi}_{n=0}^2 + \mathcal{L}_{har}^{(N-1)} + \frac{E_J}{2} \delta_m^2 \left(\frac{N-2}{N(N-1)}\right), \quad (33)$$

where $\mathcal{L}_{har}^{(N-1)}$ is defined by Eqs. (19), (20), (21) in which we have to replace N by $N - 1$. Then, from Eq. (32), one

can see that the phase θ is coupled only to the imaginary part of the modes $\varphi_k = \varphi_k^R + i\varphi_k^I$ (see Appendix A)

$$\mathcal{L}_3 = \sum_{k=1}^{k_{max}} \zeta_k \left(\frac{\hbar^2 C}{8e^2} \dot{\varphi}_k^I \dot{\theta} + \frac{E_J}{2} \varphi_k^I \theta \right), \quad (34)$$

where $k_{max} = (N-3)/2$ for N odd and $k_{max} = (N-2)/2$ for N even. We have introduced the factor ζ_k ,

$$\zeta_k = 4 \sin[2\pi k/(N-1)] / (N-1)^{1/2}. \quad (35)$$

Notice that the mode $k = 0$ is not coupled to the winding phase θ and we can omit it hereafter. The partition function associated with the total Lagrangian Eqs. (28), (29), (33), (34) reads

$$\mathcal{Z} \sim \oint \mathcal{D}[\theta(\tau)] \prod_{k=1}^{k_{max}} \oint \mathcal{D}[\varphi_k^I(\tau)] e^{-\frac{1}{\hbar} \int_0^\beta d\tau (\mathcal{L}_1 + \mathcal{L}_2 + \mathcal{L}_3)}. \quad (36)$$

It is possible to integrate out the imaginary parts of the $N - 2$ harmonic modes to obtain a single effective action describing the dynamics of θ . After the calculation, shown in Appendix A, we find

$$\mathcal{Z} \sim \mathcal{Z}_{har}^{(N-2)} \oint \mathcal{D}[\theta(\tau)] e^{-S_{eff}[\theta(\tau)]}, \quad (37)$$

where $\mathcal{Z}_{har}^{(N-2)}$ is given by Eq. (23) with $N - 1$ replacing N . After a shift of the phase $\theta \rightarrow \theta - \delta_m/N$, the effective action for the phase θ is given by

$$\begin{aligned} S_{eff} = & \int_0^\beta d\tau \left[\frac{\hbar^2}{8e^2} \left(\frac{NC}{N-1} + \frac{C_0}{2} \right) \dot{\theta}^2 - E_J \cos(\theta) + \frac{E_J(\delta_m - \theta)^2}{2(N-1)} \right] \\ & + \frac{1}{2} \int_0^\beta d\tau \int_0^\beta d\tau' G(\tau - \tau') \theta(\tau) \theta(\tau'). \end{aligned} \quad (38)$$

The effective action has a kernel $G(\tau)$ which is non-local in time and whose Fourier series is given by $G(\tau) = \sum_\ell (1/\beta) G_\ell \exp(i\omega_\ell \tau)$ where $\omega_\ell = 2\pi\ell/\beta$ are bosonic Matsubara frequencies and G_ℓ reads

$$G_\ell = \frac{\hbar^2 C_0}{4e^2} \left[\frac{\omega_\ell^2}{2(N-1)} \right] \sum_{k=1}^{k_{max}} \frac{1 + \cos\left(\frac{2\pi k}{N-1}\right)}{1 - \cos\left(\frac{2\pi k}{N-1}\right) + \frac{\pi^2}{2\lambda^2} \left(\frac{\omega_\ell^2}{\omega_\ell^2 + \omega_p^2}\right)}. \quad (39)$$

The kernel has the relevant property $G_\ell = 0$ for $\ell = \omega_\ell = 0$. The last relation is equivalent to $\int_0^\beta d\tau G(\tau - \tau') = \int_0^\beta d\tau' G(\tau - \tau') = 0$. As a consequence, this term is invariant under a shift of the winding phase $\theta \rightarrow \theta + const$. In other words, upon a proper redefinition of $G(\omega) = \omega^2 G'(\omega)$, this (kinetic) term can be written as $\sim G'(\tau - \tau') \dot{\theta}(\tau) \dot{\theta}(\tau')$.

We observe that the potential in the first line of S_{eff} in Eq. (38) corresponds exactly to the adiabatic potential $V_{eff}(\theta)$ Eq. (12) introduced in Sec. III B. This potential breaks formally the periodicity in θ in the action. This

symmetry breaking is a consequence of the fact that the QPS is a quantum tunneling in a multidimensional space with the constraint imposed by the magnetic flux threading the JJ ring (see discussion in Sec. III B).

In summary, Eqs. (37), (38), and (39) constitute the central result of this paper. They enable us to calculate the size-dependent QPS amplitude $\nu(N)$ and hence the phase-dependent ground-state energy and the ring's maximum supercurrent I_{max} in a broad range of values of the parameters N, E_J, E_C and E_0 , as we will show in detail below. However, we first establish a relation with previous work^{14,15} on infinitely long chains by considering the thermodynamic limit.

D. The thermodynamic limit and the dissipative dynamics

The effective action Eq. (38) describes the single winding junction coupled to its electromagnetic environment constituted by the other $N - 2$ junctions in the harmonic approximation. This action is very similar to the one describing the dissipative dynamics of the single Josephson junction in the framework of the Caldeira-Leggett model.³¹ In this model, an abstract bath formed by an infinite number of harmonic oscillators is phenomenologically introduced as the mechanism of irreversible loss of energy in the Josephson junction.

The external bath discussed here, expressed by the kernel $G(\tau)$ in Eq. (39), physically corresponds to the *real harmonic modes* sustained by the Josephson junction ring. These discrete modes can be experimentally designed and tested.¹² As long as the ring has finite size, there are a finite number of discrete modes and *no real dissipation* occurs. We also note that the interaction between the winding local phase-difference at the junction n_0 and these $N - 2$ harmonic modes is characterized by a linear coupling through the positions of the oscillators φ_k as well as through their velocities $\dot{\varphi}_k$, see Eq. (34). As we will show now, the difference between the system described by Eqs. (38), (39) and the standard Caldeira-Leggett model disappears in the limit $N = \infty$.

Let us consider Eqs. (38),(39). Taking the limit $N \rightarrow \infty$, the first term on the right hand side of Eq. (38) reduces to the action for a single capacitively shunted Josephson junction with a capacitance $C + C_0/2$. Equation (39) for the kernel G_ℓ then takes a simple form by replacing the sum with an integral. Proceeding in this way, we add the kinetic term of the first line of Eq. (38) to G_ℓ to recover Korshunov's result for the total kernel $\gamma(\omega_\ell)$ of a QPS in a chain of infinite length,³⁷

$$\begin{aligned} \gamma(\omega_\ell) &= \frac{\hbar^2}{4e^2} \omega_\ell^2 \left(C + \frac{C_0}{2} \right) + G_\ell \\ &= E_J \left(\frac{\omega_\ell^2}{\omega_{max}^2} \right) + \frac{\hbar\omega_\ell}{4} \sqrt{\frac{E_J}{2E_0}} \sqrt{1 + \frac{\omega_\ell^2}{\omega_{max}^2}}, \end{aligned} \quad (40)$$

where ω_{max} is defined in Eq. (22). The effective action

now reads:

$$S_{eff} = \int_0^\beta d\tau \int_0^\beta d\tau' \frac{1}{2} \gamma(\tau - \tau') \theta(\tau) \theta(\tau') - \int_0^\beta d\tau E_J \cos[\theta(\tau)]. \quad (41)$$

First, let us discuss the high and low energy regions for the dynamics of the winding phase difference θ in the cosine Josephson potential. These two regions are separated by the condition that the kinetic energy be respectively larger or smaller than the height of the potential $\sim E_J$. To estimate the kinetic energy, we determine the effective capacitance of the junction. This can be achieved by taking the limit $\omega_\ell \rightarrow \infty$. Then the kernel $\gamma(\omega_\ell)$ Eq. (40) corresponds simply to a pure capacitance

$$\gamma(\omega_\ell) \simeq \frac{(\hbar\omega_\ell)^2}{4e^2} \left(C + \frac{C_0}{4} + \sqrt{\frac{C_0}{4} \left(C + \frac{C_0}{4} \right)} \right). \quad (42)$$

The kinetic energy corresponds to the height of the potential barrier when $\gamma(\omega_\ell) = E_J$ giving the threshold $\omega_\ell = \omega_{max}$. For $\omega_\ell > \omega_{max}$ the cosine Josephson potential is a small perturbation for the dynamics θ . On the contrary, the range $\omega_\ell < \omega_{max}$ corresponds to the energy region where the winding phase θ moves well within a potential minimum. In the absence of the interaction with the modes, its dynamics is harmonic.

The threshold ω_{max} separates the low- and high-frequency part of the kernel γ Eq. (40). As we have explained, the high-frequency component $\omega_\ell > \omega_{max}$ scales approximately as $\gamma(\omega_\ell) \sim \omega_\ell^2$ and the chain behaves as a pure capacitance. On the other hand, approaching the zero frequency, $\gamma(\omega_\ell)$ scales linearly. In a Josephson junction with dissipation, this behavior corresponds to the effect of an external resistance R leading to a dimensionless damping parameter $\eta = R_q/R$ ³⁸ where $R_q = \hbar/4e^2$. In our model, for $N = \infty$, this resistance corresponds to $R = (L_J/C_0)^{1/2}$, the characteristic low-frequency impedance of the chain related to linear dispersion of the modes.

It is interesting to observe that in the standard Caldeira-Leggett model the two energy scales –the first one related to the ratio between the height of the potential and the kinetic energy and the second one related to the high-energy cut-off for the dissipation– are generally different as the latter is determined by the specific electromagnetic environment to which the junction is coupled.

Defining the relaxation time $\tau_r = RC$, we can calculate the quality factor given by the ratio between the oscillation period and the relaxation time, $Q = 2\pi/(\omega_p \tau_r) = 2\pi(C/C_0)^{1/2}$. In infinite Josephson junction chains, the underdamped regime $Q \gg 1$ corresponds thus to $C \gg C_0$.

V. RESULTS: VANISHING GROUND CAPACITANCE

We now go beyond the thermodynamic limit and discuss finite-size effects for a ring in the limit $C_0 = 0$. The non-local kernel then vanishes, $G_\ell = 0$, and the effective Lagrangian from Eq. (38) reduces to

$$\mathcal{L}_{eff} = \left(\frac{N}{N-1} \right) \frac{\hbar^2 C}{8e^2} \dot{\theta}^2 - E_J \cos(\theta) + \frac{E_J (\delta_m - \theta)^2}{2(N-1)}. \quad (43)$$

This result has a simple interpretation. Let us write the total Lagrangian, Eq. (28), with $C_0 = 0$ in terms of the phase differences θ_n ,

$$\mathcal{L} = \frac{\hbar^2 C}{8e^2} \dot{\theta}^2 - E_J \cos(\theta) + \sum_{n=1}^{N-1} \left(\frac{\hbar^2 C}{8e^2} \dot{\theta}_n^2 + \frac{E_J}{2} \theta_n^2 \right). \quad (44)$$

We observe that the phases $\{\theta_n\}$ are not coupled explicitly to the tunneling phase θ . But the total phase difference is fixed $\sum_n \theta_n + \theta = \delta_m$ which enforces an implicit interaction between them. In case of identical phase-differences θ_n for all $N-1$ junctions, we have

$$\theta_n = \frac{\delta_m - \theta}{N-1}, \quad \dot{\theta}_n = -\frac{\dot{\theta}}{N-1}. \quad (45)$$

By inserting Eq. (45) in the action Eq. (44), we obtain the effective action Eq. (43). Clearly, in the limit $N \rightarrow \infty$ finite size corrections vanish and we recover the simple action for the single JJ.

A finite value for N first of all modifies the kinetic term. The constraint-induced coupling to the other junctions increases the inertial mass C^*/C of the single phase performing an almost complete winding, leading to a reduction of the charging energy,

$$\frac{C^*}{C} = \frac{N}{N-1}, \quad \frac{E_C^*}{E_C} = 1 - \frac{1}{N}. \quad (46)$$

This causes a reduction of the QPS amplitude.

On the other hand, as we can see from Eq. (43), the action of the phase θ involves the effective adiabatic potential $V_{eff}(\theta)/E_J = 1 - \cos\theta + (\delta - \theta)^2/(N-1)/2$, see Fig. (4), which is not purely sinusoidal and depends on N , leading to additional finite-size corrections.

Before discussing these corrections, we note that for short rings, the effective potential can have only one minimum for arbitrary value of δ . This is the case, for instance, when $\delta = 0$ for $N < 5$. In this regime the harmonic approximation fails too. Focusing on lengths longer than $N \gtrsim 5$, the potential has always two minima for which the QPS process is well defined.

Due to the periodicity in δ_m and the symmetry in $(\delta_m \leftrightarrow -\delta_m)$ for the quantum ground-state of the system, we can restrict our discussion to values of δ between 0 and π ($m = 0$). In this case, the relevant tunneling process corresponds to an increase of the variable θ . The two positions corresponding to the two minima

of the effective potential are, respectively, $\theta_l = \delta/N$ and $\theta_r = 2\pi + (\delta - 2\pi)/N$, with the energies $V_{eff}(\theta_l)$ and $V_{eff}(\theta_r)$ which correspond to the two classical energies associated with the initial state and the final state before and after a QPS, respectively.

A. Symmetric effective potential ($q < 1$)

For small values of the parameter q , Eq. (14), the hopping term is small, Eq. (13). The QPS process couples mainly two neighboring classical states, $|m\rangle$ and $|m+1\rangle$, and it is significant when they are degenerate. This occurs for $\delta \simeq \pi$ which corresponds to the point of the maximum of the supercurrent in this regime (Fig. 5).

Therefore, we start by discussing the case $\delta = \pi$ when the effective potential $V_{eff}(\theta)$ is symmetric around the maximum, Fig. (4). Then the effective potential is very well approximated by a renormalized cosine potential of the form $-E_J^* \cos[\theta(N-1)/N]$ (see inset Fig. 4) where E_J^* is the renormalized Josephson energy (half of the height of the energy barrier separating the two wells),

$$\frac{E_J^*}{E_J} = \frac{1}{2} \left[1 + \cos\left(\frac{\pi}{N}\right) - \frac{\pi^2}{2N^2} (N-1) \right] \simeq 1 - \frac{\pi^2}{4N}. \quad (47)$$

The ratio E_J^*/E_J is an increasing function of N which converges to one in the limit of $N \gg 1$. Thus for any finite-size system, this correction corresponds to a decrease of the barrier for quantum tunneling which therefore would lead to an enhancement of the QPS amplitude, in contrast to the effect of the renormalized capacitance, Eq. (46). Another effect which enhances the tunneling amplitude is the reduction of the distance between the two minima of the effective potential,

$$\frac{\Delta\theta^*}{2\pi} = 1 - \frac{1}{N}, \quad (48)$$

contributing to the enhancement of the tunneling amplitude for finite N . Similar renormalization effects have been discussed in Ref. 28, albeit for different superconducting circuits.

The three different effects given by Eqs. (46), (47), (48) combine in the final expression for the renormalized effective amplitude for the quantum tunneling between the two degenerate minima,

$$\nu(N) = \sqrt{\left(\frac{2\pi}{\Delta\theta^*}\right)} \frac{4}{\sqrt{\pi}} (8E_J^* E_C^*)^{\frac{1}{4}} e^{-\left(\frac{\Delta\theta^*}{2\pi}\right)} \sqrt{8\frac{E_J^*}{E_C^*}}. \quad (49)$$

For the range of interest $N \geq 5$, the QPS amplitude Eq. (49) decreases with the length N indicating that the latter effects (reduced barrier height and distance between minima) dominate the capacitance renormalization. Indeed, when ν is scaled with the amplitude ν_0 (corresponding to the limit $N = \infty$), the leading exponential term reads $\nu/\nu_0 \sim \exp(N_c/N)$ with $N_c = (\pi^2 + 4)\sqrt{8E_J/E_C}$. Here N_c is the typical length below

which this finite size correction becomes relevant. The behavior of the ratio ν/ν_0 is shown in Fig. 7.

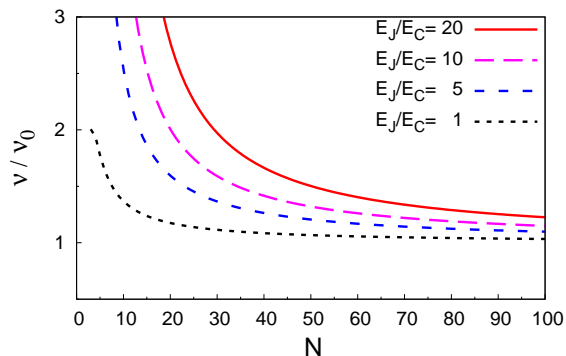


Figure 7: For $C_0 = 0$, the renormalized QPS amplitude ν as a function of N , Eq. (49), scaled with ν_0 , Eq. (1), for different values of the ratio E_J/E_C .

The effective QPS amplitude ν decreases with increasing N . As a result the parameter $q \sim N^2\nu(N)$ defined in Eq. (14) has a non-monotonic behavior as a function of N . Accordingly, the maximum supercurrent obtained for Eq. (13) has also a non-monotonic dependence on the total length N . In Fig. 8 we show the maximum supercurrent as a function of the ring size N for different ratios of E_J/E_C . Decreasing E_J/E_C , the non-monotonic behavior occurs at shorter lengths.

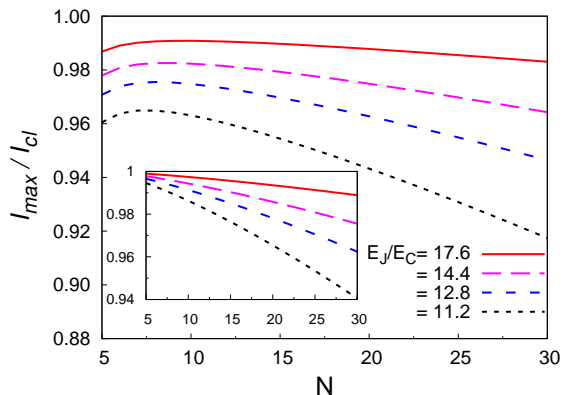


Figure 8: The maximum supercurrent I_{max} scaled with I_{cl} as a function of N and at different values of the ratio E_J/E_C by using the QPS amplitude $\nu(N)$ Eq. (49). Inset: the maximum supercurrent by using the QPS amplitude ν_0 , Eq. (1).

B. Asymmetric effective potential ($q \gtrsim 1$)

When the parameter q is of order ~ 1 , the maximum supercurrent for the model given by Eq. (13) shifts from the phase difference $\delta = \pi$ to the phase difference $\delta = \pi/2$, Fig. 5. The current-phase relation is strongly modified passing from a sawtooth to a sinusoidal function.²⁴ We should then solve Eq. (13) using

the renormalized QPS amplitude ν_{as} associated with the full asymmetric effective potential V_{eff} and which depends on δ , Fig. 4.

To reach the regime $q \gtrsim 1$ there are two possible ways. First, it can be reached by decreasing the ratio E_J/E_C at given fixed length N , which is outside the range of validity of the present work. Alternatively, for a given ratio E_J/E_C , we can increase the length N of the system. The finite size effects that we have discussed in the previous section for the phase difference $\delta = \pi$ vanish as $1/N$. We now show that the finite-size corrections due to the asymmetry of the barrier vanish more rapidly, namely as $1/N^2$. Consequently, in the cross-over range in which N spans from $N_{min} = 6$ to $N \gg 1$, we can neglect the difference between ν_{as} (for $\delta \neq \pi$) and ν (for $\delta = \pi$). It is then justified to use the renormalized amplitude ν for the symmetric potential, Eq. (49), when calculating the maximum supercurrent for the model Eq. (13) in the full range of q .

Let us introduce $\kappa = 1 - \delta/\pi$ as the natural parameter to quantify the asymmetry. For an asymmetric potential, we can approximate the hopping energy between the two levels as the geometrical average obtained by considering the hopping for the left part of the potential and the right part of the potential with respect to the maximum,^{39,40}

$$\nu \simeq \sqrt{\nu_L \nu_R}. \quad (50)$$

The left (right) amplitude ν_L (ν_R) is the tunneling amplitude for the symmetric double potential, Eq. (49), with the barrier height $2E_J^{(+)}$ ($2E_J^{(-)}$) given by the difference between the maximum energy and the left (right) minimum. In a similar way, $\Delta\theta^{(\pm)}/2\pi$ is the distance between the maximum and the left (right) minimum point. Keeping the leading term of the expansion in $1/N$, they read $E_J^{(\pm)}/E_J = 1 - (\pi^2/4N) \pm (\pi^2/2N)\kappa$ and $\Delta\theta^{(\pm)}/2\pi = 1 - 1/N \pm (\pi/N)\kappa$ where \pm is for L and R . Inserting this expansion into Eq. (50), we finally conclude that finite-size corrections associated with the asymmetry parameter κ cancel at order $1/N$. When higher-order corrections are taken into account by using the full formula Eq. (50) for the QPS amplitude $\nu = \nu(\delta)$, the differences with the amplitude at $\nu = \nu(\pi)$ are practically unnoticeable.

Finally, our discussion is valid in the limit in which the asymmetry is sufficiently weak such that the two level description remains valid. Close to the resonant condition, the excited and ground harmonic levels between two neighboring states in the effective potential, Fig. 4, are almost degenerate. This implies the inequality $E_n - E_{n+1} < \hbar\omega_p$ which translates into an interval for the magnetic flux $|\Delta\delta| < N\sqrt{2E_C/E_J}/\pi$ around the degeneracy point at half a flux quantum. As long as the maximum supercurrent is well within this interval, our analysis based on the simple two level description holds. Note that in the limit $N \rightarrow \infty$, the range $|\Delta\delta|$ is quite large as a consequence of the fact that V_{eff} in Fig. 4 is practically indistinguishable from the periodic and multi-degenerate cosine potential. On the other hand, for short

rings, the maximum supercurrent occurs around $\delta \simeq \pi$, Fig. 5, which is well inside the interval $|\Delta\delta|$ for a suitable choice of the parameters.

VI. EFFECTS OF THE CAPACITANCE C_0

We now consider the effect of the ground capacitance C_0 on the QPS amplitude. In view of the discussion of the previous section, we will focus on the analysis of the case $\delta = \pi$. Then the effective potential appearing in the first line of Eq. (38) is replaced by a renormalized cosine potential

$$S_{eff} = \int_0^\beta d\tau \left[\frac{\hbar^2}{8e^2} \left(C^* + \frac{C_0}{2} \right) \dot{\theta}^2(\tau) - E_J^* \cos \left(\frac{2\pi}{\Delta\theta^*} \theta(\tau) \right) \right] + \frac{1}{2} \int_0^\beta d\tau \int_0^\beta d\tau' G(\tau - \tau') \theta(\tau) \theta(\tau'), \quad (51)$$

where C^* , E_J^* are defined in Eqs. (46,47) and $\Delta\theta^*$ in Eq. (48). Within the semiclassical instanton approach,⁴¹ the QPS amplitude reads

$$\nu = A \exp \left[-S_{eff}^{(cl)} / \hbar \right], \quad (52)$$

where $S_{eff}^{(cl)}$ is the effective action Eq. (51) evaluated at $\theta_{cl}(\tau)$, the asymptotic path which minimizes the action and which connects the two relevant minima in the limit $\beta \rightarrow \infty$, *i.e.*, the instanton solution. The prefactor A is related to the quantum fluctuations around this minimum path.⁴¹

In contrast with the previous analysis for $C_0 = 0$, we now have to take into account the effects of the kernel $G(\tau)$ in the action Eq. (51).

A. Parabolic approximation

The first step is to find the classical path $\theta_{cl}(\tau)$. For a cosine-potential, this solution is known analytically only when the kernel is zero $G(\tau) = 0$ ($C_0 = 0$). For the general case, to the best of our knowledge, the solution is unknown. We use the Villain approximation to solve the problem.⁴² We replace the periodic cosine potential by a parabolic potential

$$S_p = \int_{-\frac{\beta}{2}}^{\frac{\beta}{2}} d\tau \left[\frac{\hbar^2}{8e^2} \left(C^* + \frac{C_0}{2} \right) \dot{\theta}^2 + \frac{V_J}{2} \min(\theta - m \Delta\theta^*)^2 \right] + \frac{1}{2} \int_{-\frac{\beta}{2}}^{\frac{\beta}{2}} d\tau \int_{-\frac{\beta}{2}}^{\frac{\beta}{2}} d\tau' G(\tau - \tau') \theta(\tau) \theta(\tau'). \quad (53)$$

It is worth noting that, for $G = 0$ ($C_0 = 0$) and $N \gg 1$, the instanton solution for this potential yields the action $S_{eff}^{(cl)} / \hbar = \pi^2 (V_J / 8E_C)^{1/2}$, *i.e.*, the numerical coefficient is different from the one found for a cosine potential with the same amplitude V_J . Thus, in order to recover the

previous results for $C_0 = 0$, it is convenient to set the height of the parabolic periodic potential to the value $V_J = (8/\pi^2)^2 E_J^*$ to take into account the difference between the profiles of the two potentials.

After the calculation (see Appendix B for details), the action Eq. (53) with the instanton path reads⁴³

$$S_p^{(cl)} = 2\pi V_J \left(1 - \frac{1}{N} \right)^2 \int_0^\infty d\omega \frac{1}{\omega^2 + \frac{4e^2 V_J / \hbar^2}{C^* + \frac{1}{2} C_0 + \frac{4e^2}{(\hbar\omega)^2} G(\omega)}}, \quad (54)$$

where $G(\omega)$ is the continuous limit for the Fourier transform $G(\omega_\ell) = G_\ell$ defined in Eq. (39). In Fig. 9, the behavior of $S_p^{(cl)}$ is shown as a function of the ring size N . For $C_0 = 0$ and $N \gg 1$, $S_p^{(cl)}$ saturates to $S_0 = (8E_J/E_C)^{1/2}$. When the ground capacitance is restored, we find a logarithmic scaling with N for $N > \lambda$. Specifically, we find that $\nu \sim \exp[-\alpha \log(N)] = 1/N^\alpha$ with $\alpha = \pi \sqrt{E_J / (8E_0)}$ (see Appendix C).

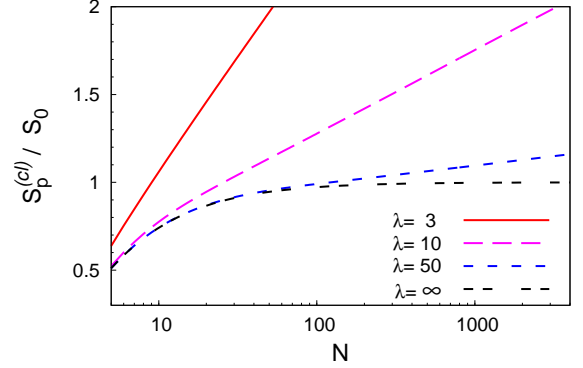


Figure 9: For $E_J = 8E_C$, the classical action $S_p^{(cl)}$ Eq. (54) scaled with $S_0 = (8E_J/E_C)^{1/2}$ as a function of N for different screening lengths $\lambda = 3, 10, 50, \infty$. Notice the cross-over at $N \gtrsim \lambda$ to the logarithmic scaling $\sim \log(N)$.

B. The prefactor A

So far our semiclassical approach was general. We will now restrict ourselves to the calculation of the finite-size corrections entering the renormalized amplitude ν with exponential accuracy; this corresponds to the leading dependence on N . Correspondingly, we will use an approximate expression for the prefactor A . This prefactor is associated with the quantum Gaussian fluctuations around the classical path. Specifically, we neglect the contribution of the low energy paths having a mean kinetic energy lower than the height of the potential.

Proceeding as in Sec. IV D, to estimate the kinetic energy we determine the effective capacitance of the junction in the ring but now taking into account the finite size effects. For $\omega_\ell \rightarrow \infty$ the kernel Eq. (39) reduces to

$G_\ell = \Delta C(\hbar\omega_\ell)^2/(4e^2)$ where

$$\Delta C = \frac{C_0}{2(N-1)} \sum_{k=1}^{k_{max}} \frac{1 + \cos\left(\frac{2\pi k}{N-1}\right)}{1 - \cos\left(\frac{2\pi k}{N-1}\right) + \frac{\pi^2}{2\lambda^2}}, \quad (55)$$

so that the effective capacitance of the junction corresponds to

$$C_{eff} = C^* + \frac{1}{2}C_0 + \Delta C. \quad (56)$$

Again, from Eq. (53), as $V_J \sim E_J$ we see that the threshold frequency separating the high and low energy regions is still $\omega_\ell = \omega_{max}$ for $C > C_0$. From these observations, in order to take into account the contribution of the high energy quantum fluctuations, we replace the effective capacitance in the prefactor A of Eq. (49) (case $C_0 = 0$), with the effective capacitance Eq. (56). The result reads

$$A = \frac{4}{\sqrt{\pi}} \sqrt{\left(\frac{2\pi}{\Delta\theta^*}\right)} \left(8E_J^{*3} \frac{e^2}{2C_{eff}}\right)^{\frac{1}{4}}. \quad (57)$$

We now discuss the conditions for this approximation to be valid. For $\omega_\ell < \omega_{max}$ the kernel G in Eq. (53) couples the dynamics of the winding phase to the one of the modes. As we have seen at the end of Sec. IV D at $N = \infty$, for $C \gg C_0$ this interaction between the winding phase and the modes corresponds to a perturbation at low energies for the Gaussian harmonic fluctuations. Indeed, at $N = \infty$ we have weak damping for the quality factor $Q = 2\pi(C/C_0)^{1/2} \gg 1$. Although at finite N the dynamics of the JJ ring does not correspond to a real resistance, the ratio C_0/C still plays the role of a dimensionless coupling between the winding phase and the harmonic bath. The effect of this interaction on the low energy Gaussian fluctuations can be neglected in the prefactor but not in the exponent where, as we have seen, they strongly affect the instanton classical path.

C. Superconductor-Insulator transition

By inserting Eq. (54) and Eq. (57) into Eq. (52), we obtain the QPS amplitude which we use to calculate the maximum supercurrent. Here we discuss some numerical results valid in a general range of parameters while in Appendix C we discuss some analytic results valid for very long chains ($N \gg \lambda$).

In Fig. 10, we plot the factor $q = N^2\nu(N)/(2\pi^2)$ as a function of the ring size N for the values $C = 2C_0$ and for different ratios of E_J/E_C . In the inset of Fig. 10 we also show the behavior of ν/E_J . The first striking observation is that for large ratios of $E_J/E_C = 2(E_J/E_0)$, the parameter q does not increase as N^2 but, indeed, it vanishes upon increasing the length. This is due to the logarithmic dependence of the action S_{eff} that we have obtained in Sec. VI A.

The presence of the logarithmic dependence is related to the lowest energy modes (see Appendix C). Indeed, below the corresponding threshold $\omega_\ell \ll \omega_{min}$, the winding junction feels the discreteness of the spectrum of the environment with which it can exchange energy. It is equivalent to say that there is no real dissipation at low frequency. An instanton solution conserving the initial energy still exists with a finite value of the corresponding action. For $N \gg \lambda$, we have $\omega_{min} \sim (8E_J E_0)^{1/2} \pi/N$. Eventually, ω_{min} vanishes as $N \rightarrow \infty$ and the action associated to the instanton diverges.

As a consequence, the parameter q behaves as $q \sim N^{2\nu} \sim N^{2-\alpha}$ and it scales either to zero or to infinity for $N = \infty$. A cross-over is therefore expected at some critical ratio E_J/E_0 as $\alpha = \pi\sqrt{E_J/(8E_0)}$ (see Appendix C).

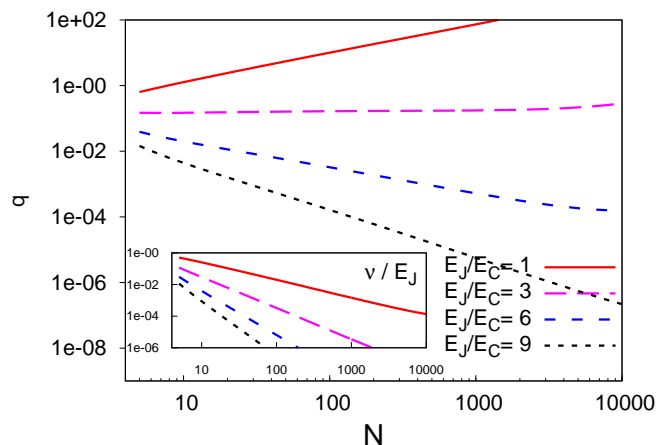


Figure 10: The parameter q as a function of N for $C = 2C_0$ and different ratios E_J/E_C . Inset: the behavior of the QPS amplitude ν scaled with E_J .

The behavior of the maximum supercurrent I_{max} scaled with I_{c1} as a function of N , Fig. 11, is related to the behavior of q . In the very long length limit, I_{max}/I_{c1} increases and saturates to one for $E_J/E_0 > 3.24$ whereas for $E_J/E_0 < 3.24$ it vanishes. On the other hand, we remark that for finite systems, the current shows a non-monotonic behavior: it increases with N up to a maximum after which it decreases.

The interplay between finite size effects, which scale as $\nu(N) \sim \exp(N_c/N)$, and the low energy modes at finite C_0 , which reduce the QPS amplitude as $\nu \sim 1/N^\alpha$, cause that the total QPS amplitude of the ring $\nu_{ring} = N\nu(N)$ has a weak N -dependence so that the dependence of the maximum supercurrent on N appears almost flat over a large range of N when the critical ratio is approached (see Fig. 11).

Due to the non-monotonicity of the current as a function of N , the critical point between the superconducting phase and the insulator phase can be better determined by plotting the maximal supercurrent as a function of the ratio E_J/E_C for different circumferences. The result is shown in Fig. 12 for the case $C = 2C_0$.

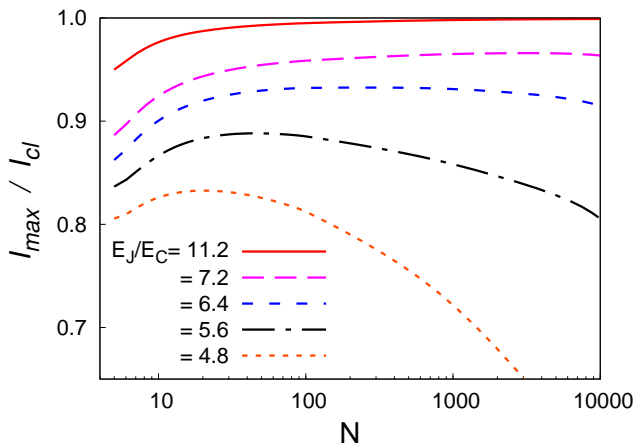


Figure 11: The maximum supercurrent I_{max} scaled with the classical value I_{cl} as a function of N for $C = 2C_0$ and different ratios E_J/E_C .

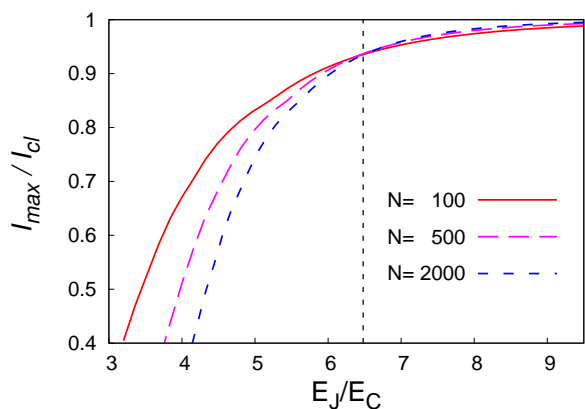


Figure 12: I_{max} scaled with I_{cl} as a function of $E_J/E_C = 2E_J/E_0$ for rings of different circumferences. The dashed vertical line corresponds to the critical value $E_J/E_0 = 32/\pi^2$ of Ref. 15 for $C = 2C_0$.

We find that the critical value saturates to the value $E_J/E_0 \simeq 3.24$, as long as $C \geq 2C_0$. This result is in agreement with the result obtained by Korshunov¹⁵ who calculated $E_J/E_0 = 32/\pi^2$ in the regime $C \gg C_0$. Reducing the ratio C/C_0 , we find a small increase of the critical value E_J/E_0 which saturates to ~ 4.16 for vanishing mutual capacitance $C = 0$. In this limit, we do not recover the critical ratio $E_J/E_0 = 128/\pi^2$ obtained by Bradley and Doniach.¹³

D. Discussion

In this section we discuss the validity of the single QPS approximation.

a. The case $C_0 = 0$. In this case, it is most convenient to express the Lagrangian in terms of the phase

differences $\{\theta_n\}$,

$$\mathcal{L} = \sum_n \left[\frac{\hbar^2 C}{8e^2} \dot{\theta}_n^2 - E_J \cos \left(\theta_n + \frac{\delta}{N} \right) \right], \quad (58)$$

showing that there is no correlation in the spatial direction. Indeed, Eq. (58) with the constraint Eq. (3) describes $N - 1$ independent variables. Under the condition $E_J > E_C$ one therefore can use the semiclassical instanton approach to describe the QPS in each individual junction. This is a well-controlled technique,⁴¹ based on the non-interacting (dilute) instanton approximation. For instance, in the limit $N \gg 1$, the problem reduces to the tunneling of a free particle in a double-well. The resulting tunnel amplitude is ν_0 , Eq. (1), which is independent of the size of the system. The total amplitude $N\nu_0$ grows linearly with N since instantons which can occur independently in any of the junctions, as previously analyzed in Ref. 24. The system becomes an insulator for $N \rightarrow \infty$; no phase transition occurs, in agreement with conclusions obtained in the thermodynamic limit.¹³⁻¹⁵

b. The case $C_0 \ll C$ and $N \lesssim \lambda$. When C_0 is restored, an interaction appears between the phase-differences $\{\theta_n\}$.¹⁴ This interaction yields a possible coupling between QPSs occurring in different junctions $n \neq m$. This bare interaction is proportional to C_0/C . For finite systems and for $C_0 \ll C$ we expect that, by continuity with the case $C_0 = 0$, this interaction can be neglected in first approximation. Indeed, the instantons are still rare events in the imaginary time for $E_J \gg E_C$ so that one can study a single instanton centered in one junction θ_{n_0} . The other phase-differences $n \neq N - 1$ can be approximated by $N - 2$ harmonic oscillators coupled to the winding phase θ_{n_0} .

Another consequence of a finite C_0 is the fact that the modes have a frequency dispersion. This leads to an additional non-local term in the effective action of θ_{n_0} , Eq. (51), beyond the finite-size corrections discussed for the case $C_0 = 0$. In particular we considered the adiabatic regime in which all the modes have a frequency higher than the tunneling frequency of the phase θ_{n_0} . This situation is very close to the case $C_0 = 0$: the quantum tunneling of a fictitious particle in a double-well can be still reduced to the tunneling between two levels but with an adiabatically renormalized amplitude. This is exactly the theoretical framework presented in Ref. 44, in which the authors developed the analysis for a generic two-level system. In particular they considered the adiabatic regime expressed by their Eq. (2.9) which corresponds to our Eq. (52). We exploited this approach for a specific system, namely the Josephson junction ring threaded by a magnetic flux. Moreover, as shown in Sec. VI and in Appendix C, the corrections to the instanton action due to the non-local term are small as long as $N \lesssim \lambda$. Therefore, by continuity to the previous case, we expect that our results are qualitatively and quantitatively correct in this regime.

c. The case $C_0 \ll C$ and $N \gg \lambda$. In the opposite limit $N \gg \lambda > 1$ (see Appendix C), we find a logarithmic

dependence on N for the leading term in the instanton action $S_p^{(cl)} \sim \pi\sqrt{E_J/(8E_0)}\log(N/\lambda)$. Approaching the thermodynamic limit ($N \rightarrow \infty$), even for $C_0 \ll C$, the ground capacitance C_0 has a substantial effect. It leads to a renormalized QPS amplitude which strongly depends on the length of the JJ ring $\nu \sim \nu_0 N^{-\sqrt{\pi^2 E_J/(8E_0)}}$.

The validity of this result is addressed in the next subsection.

E. The relation with the BKT transition.

Mathematically, the one-dimensional quantum model of the type in Eq. (2) can be mapped onto a two-dimensional classical model. Considering the axis $x = \tau$ (imaginary time) and the axis $y = n$ (position on the chain) for the local phases $\{\varphi_n(\tau)\}$, Bradley and Doniach showed that, for the case $C = 0$, the 1D JJ chain is equivalent to an anisotropic 2D classical spins with nearest neighbors interactions along the perpendicular axis.¹³

Hence, according to this mapping, the superconductor-insulator phase transition occurring in the case $N = \infty$ corresponds to the order-disorder phase transition of an ensemble of ferromagnetically coupled planar classical spins. This is the celebrated Berezinskii-Kosterlitz-Thouless (BKT) transition, marked by a disruption of the ordered ferromagnetic phase due to the appearance of vorticity: topological defects for which the spin orientation changes by 2π when following a closed path around them once. Reducing the ratio E_J/E_0 , the BKT-transition is driven by the dissociation of bound vortex – anti-vortex pairs formed in the ordered phase for the local phases $\{\varphi_n(\tau)\}$.¹³ Thus, as interaction between vortices plays an essential role in this scenario, a natural question is the range of validity of our approach where the correlations between QPSs have been ignored.

Korshunov in Ref.14 analyzed the same problem ($C = 0$) but using the representation in the space of the phase-difference $\{\theta_n(\tau)\}$. In this space, the relevant (non-linear) quantum fluctuation are the instantons, *i.e.*, the QPSs. Notice that the vortices and the QPSs are not exactly the same object: the former are configurations defined in the space of the local phase $\{\varphi_n(\tau)\}$ of the BCS condensate in each superconducting island¹³ whereas the latter are defined in the space of the phase differences $\{\theta_n(\tau)\}$ in each Josephson junction.¹⁴

The two instantons defined the θ -space interact as¹⁴

$$\mathcal{S}_{int}(\tau, \Delta N) \sim \pi\sqrt{E_J/E_0} \log \left[(\omega_0\tau)^2 + \Delta N^2 \right], \quad (59)$$

in which $\omega_0 \sim (E_J E_0)^{1/2}$ and $(\tau, \Delta N)$ are the separation along the imaginary time axis and in real space, respectively. Remarkably, two instantons interact again with a logarithmic potential in the two directions in a very similar way to the vortices defined the φ -space. This interaction leads to the formation of bound-pair states of QPSs which makes the superconducting phase stable, even for an infinite number of QPSs.

This implies that, even if we focus on an individual junction ($\Delta N = 0$), interaction appears between different instantons along the imaginary time.

The crucial point is that this interaction is mediated by the propagating modes on the loop and is present only in the thermodynamic limit $N = \infty$, when the modes are sufficiently dense.⁴⁴ In this limit, the local junction hosting a QPS is coupled to the rest of the infinite chain which acts as a dissipative environment. Indeed, the other Josephson junctions form a *dense* bath of harmonic oscillators with linear low-frequency dispersion. They mediate the interactions of two different instantons in imaginary time. This is the reason for the appearance of non-local correlations in time between different instantons. As discussed in Sec. IV D, the ratio C_0/C plays the role of coupling between the winding phase and the harmonic bath of oscillators formed by the other $N-1$ junctions. Although the coupling constant is small ($C_0 \ll C$), the dynamics of the winding phase is now dissipative and the instantons in imaginary time are strongly coupled with a long-range logarithmic potential: the single QPS approximation breaks down.

As long as N remains finite, no real dissipation appears and therefore no logarithmic interaction between instantons occurs in imaginary time. In particular we studied the adiabatic regime in which the problem can be reduced to the renormalized quantum tunneling of a fictitious particle in a double-well potential⁴⁴ (see the cases *b* and *c* in Sec. VI D).

Between these two limits, we have a continuous crossover from the adiabatic regime to the full dissipative dynamics at $N = \infty$. Therefore we expect that, at given ratio C/C_0 and E_J/E_C , there is a typical length N^* which sets an upper bound for the range of validity of the single QPS approximation.

Indeed, increasing the length N , the lowest frequency ω_{min} defined in Eq. (25) decreases as $\hbar\omega_{min} \sim 4\sqrt{2E_J E_C}(\lambda/N)$. Then, for our approach to be self-consistent, we estimate N^* as the point at which the adiabatic condition breaks down, namely when the level splitting of the two level system coincides with the lowest frequency of the modes: $2\nu_0 \sim \hbar\omega_{min}$. It gives

$$N^*/\lambda = (\sqrt{\pi}/2^{3/4}) e^{\sqrt{8\frac{E_J}{E_C}}}/(E_J/E_C)^{1/4}. \quad (60)$$

As an example, at $E_J/E_C = 6.5$, $\lambda = 4.4$, ($C = 2C_0$) (the values close to the phase-transition, see Fig. 12) we have the condition $N^* \sim 2800$.

For $N \gtrsim N^*$ only a finite number of discrete modes have frequencies lower than the tunneling frequency.⁴⁵ Notice that this region beyond $N \gtrsim N^*$ is still far away from the full dissipative limit $N = \infty$, in which we expect a logarithmic interaction between instantons Eq. (59). Therefore one has to consider Eq. (60) as a rough estimate. Remarkably, as shown in Fig. 12, in finite-size systems with $N \sim 10^3$ and well below the line $N = \infty$, the crossing point of the maximal current can be very close to the critical value of the phase-transition although the

current does not drop vertically to zero as expected in the real thermodynamic limit.

We conclude by recalling that the exact analysis of the interaction between two instantons in imaginary time beyond the limit $N \gg N^*$ in JJ chains is an interesting and open theoretical issue, beyond the aim of the present work. Moreover we remark that the Lagrangian of Eq. (16) can be exactly mapped on the classical (anisotropic) XY spin-Hamiltonian – which represents the reference model for the BKT transition – only for $C = 0$. For the general case of (C, C_0) , the two-dimensional classical spin Hamiltonian associated with the Lagrangian of Eq. (16) has a four-body anisotropic-diagonal interaction between the spins $\varphi_n(\tau)$. Even at $N = \infty$, the superconductor/insulator transition in the extreme regime $C \gg C_0$ has not yet been analyzed in detail in the literature (with the exception of Ref. 15).

VII. SUMMARY AND CONCLUSIONS

In this work we studied the quantum QPS processes in 1D Josephson junction rings in the strong Josephson coupling limit $E_J \gg E_C, E_0$. In contrast with the previous work,²⁴ we consider JJ rings of finite size in a wide range of lengths ($N \gtrsim 5$) and with ground capacitance C_0 . We calculated the renormalized QPS amplitude $\nu(N)$ and we discussed its consequence for the maximum supercurrent I_{max} flowing through a JJ ring threaded by a magnetic flux.

For the case $C_0 = 0$, we found an interplay between different finite-size effects which gives rise to a non-monotonic behavior of the maximum supercurrent I_{max}/I_{cl} as a function of the ring size. The critical length above which finite size corrections are negligible is $N_c \sim (\pi^2 + 4)\sqrt{8E_J/E_C}$.

When the ground capacitance is restored, $C_0 > 0$, dispersive modes are possible on the ring which are directly coupled to the local winding phase-difference. When $N \rightarrow \infty$ we found that the system converges either to a superconducting state with $I_{max}/I_{cl} = 1$ or to an insulating phase $I_{max}/I_{cl} = 0$, depending on the ratio E_J/E_0 . For $C > C_0$ we found as critical ratio $(E_J/E_0)_c = 3.24$, in agreement with the previous work of Ref. 15.

Although our analysis was mainly developed for a ring of identical junctions, it is also relevant for other systems, for instance for a weak winding junction coupled to a chain of Josephson junctions in which the QPS is prevented, *i.e.*, the so-called fluxonium.¹¹

We have discussed the validity of the single QPS approximation. The regime $E_C > E_J$ associated with the regime of strong interaction between the QPSs is beyond the scope of this article. A global phase diagram was reported some time ago in Refs. 14,15 in the thermodynamic limit but it was based on a perturbative renormalization group analysis. A phase-diagram obtained by non-perturbative approaches as well as the behavior of finite-size systems for arbitrary ranges of the parameters

E_J, E_0, E_C and C/C_0 constitutes a still open theoretical issue.

Acknowledgments

We thank W. Guichard, L. Glazman, M. Vanević, L. Amico and L. Ioffe for useful discussions. This work was supported by ANR through contracts DYCOSMA and QUANTJO. We acknowledge support from the European networks MIDAS, SOLID and GEOMDISS and from Institut universitaire de France.

Appendix A: Path integral

In this Appendix we summarize the main steps for the calculation of the path integral Eq. (36).

First we recall that any periodic function φ_n on the lattice $n = 0, \dots, N - 1$ can be decomposed as Eq. (18) where the set $\{\varphi_k\}$ are complex numbers, *i.e.*, $\varphi_k = \varphi_k^R + i\varphi_k^I$. They are related by the condition $\varphi_{N-k} = \varphi_k^*$ as φ_n is real. Using this property, we can write

$$\varphi_n = \frac{1}{\sqrt{N}} \left[\varphi_{k=0} + \underbrace{(-1)^n \varphi_{k=\frac{N}{2}}}_{N \text{ even}} + \sum_{k=1}^{k_{max}} \left(\varphi_k e^{i\frac{2\pi k}{N}n} + c.c. \right) \right]. \quad (\text{A1})$$

For N even we have $k_{max} = (N/2) - 1$ whereas for N odd we have $k_{max} = (N-1)/2$. We can express the Euclidean Lagrangians only in terms of the independent variables. Setting the action

$$L_0(x_k) = \frac{1}{2} \mu_k \dot{x}_k^2 + \frac{1}{2} \mu_k \omega_k^2 x_k^2, \quad (\text{A2})$$

one can demonstrate that the harmonic Lagrangian Eq. (17) (omitting the constant proportional to δ_m) in terms of the modes k reads

$$L_0^{(N)} = \frac{\mu_0}{2} \dot{\varphi}_{k=0}^2 + \underbrace{L_0(\varphi_{k=\frac{N}{2}})}_{N \text{ even}} + 2 \sum_{k=1}^{k_{max}} [L_0(\varphi_k^R) + L_0(\varphi_k^I)]. \quad (\text{A3})$$

We now consider the actions Eqs. (29), (31), and (32) where we have $N - 1$ harmonic variables φ_n .

Inserting Eq. (A1) with N replaced by $N - 1$ in Eq. (32), one can obtain that only the imaginary parts of the modes are linearly coupled to external forces $(\theta(\tau), \dot{\theta}(\tau))$ through the position and through the velocity, *i.e.*, Eq. (34). For the notation we set

$$q_k(\tau) \equiv \varphi_k^I(\tau), \quad (\text{A4})$$

and we can write

$$\mathcal{L}_3 = \sum_{k=1}^{k_{max}} \zeta_k \left(\frac{\hbar^2 C}{8e^2} \dot{q}_k \dot{\theta} + \frac{E_J}{2} q_k \theta \right). \quad (\text{A5})$$

From Eq. (A1) we observe that the phase $\varphi_{n=0}$ at $n = 0$ depends only on the real part of the mode $\{\varphi_k^R\}$. Therefore the first term of Eq. (31), $\varphi_{n=0}^2$, couples only the real parts of the different modes k . As real and imaginary part are decoupled, the relevant term in Eq. (33) in which we are interested for the calculation of the effective action reduces to

$$\mathcal{L}_2 \sim \mathcal{E}_0 + 2 \sum_{k=1}^{k_{max}} \left(\frac{1}{2} \mu_k \dot{q}_k^2 + \frac{1}{2} \mu_k \omega_k^2 q_k^2 \right), \quad (\text{A6})$$

with $\mathcal{E}_0 = E_J \delta_m^2 (N-1)/(2N^2)$. We express the generic periodic path of the partition function as

$$q_k(\tau) = q_{k,0} + \sum_{\ell=1}^{+\infty} (q_{k,\ell} e^{i\omega_\ell \tau} + c.c.), \quad (\text{A7})$$

in which the Fourier (Matsubara) component at $\omega_\ell = 2\pi\ell/\beta$ is given by $q_{k,\ell} = (1/\beta) \int_0^\beta d\tau \exp(-i\omega_\ell \tau) q_k(\tau)$. Inserting the expression Eq. (A7) into the Lagrangian $\mathcal{L}_2 + \mathcal{L}_3$ Eqs. (A5),(A6) and integrating over the time, we obtain

$$\int_0^\beta d\tau (\mathcal{L}_2 + \mathcal{L}_3) = \mathcal{E}_0 + 2 \sum_{k=1}^{k_{max}} \left(\mathcal{S}_{k,0} + \sum_{\ell=1}^{+\infty} \mathcal{S}_{k,\ell} \right). \quad (\text{A8})$$

The first term $\mathcal{S}_{k,0}$ contains only the component at zero frequency of $\theta(\tau)$ and $q_k(\tau)$,

$$\mathcal{S}_{k,0} = \frac{\beta}{2} \mu_k \omega_k^2 q_{k,0}^2 + \frac{\beta E_J}{2} q_{k,0} \theta_0. \quad (\text{A9})$$

The second terms $\mathcal{S}_{k,\ell}$ contain all the nonzero frequency components ($\ell > 0$)

$$\mathcal{S}_{k,\ell} = \beta \mu_k (\omega_\ell^2 + \omega_k^2) |q_{k,\ell}|^2 + \frac{\beta \zeta_k \hbar^2}{16 E_C} (\omega_\ell^2 + \omega_p^2) (q_{k,\ell}^* \theta_\ell + c.c.) \quad (\text{A10})$$

Finally, the path integral is evaluated by integration over the Fourier components as

$$\begin{aligned} \Delta \mathcal{Z} &= \prod_{k=1}^{k_{max}} \int \mathcal{D}[q_k(\tau)] e^{-\frac{1}{\hbar} \int_0^\beta d\tau (\mathcal{L}_2 + \mathcal{L}_3)} = e^{-\frac{\beta \mathcal{E}_0}{\hbar}} \\ &\times \prod_{k=1}^{k_{max}} \int \frac{dq_{k,0}}{\sqrt{\frac{4\pi\beta\hbar}{\mu_k}}} e^{-\frac{2\mathcal{S}_{k,0}}{\hbar}} \prod_{\ell=1}^{+\infty} \iint \frac{dq_{k,\ell}^R dq_{k,\ell}^I}{\frac{\pi\hbar}{\beta\mu_k\omega_\ell^2}} e^{-\frac{2\mathcal{S}_{k,\ell}}{\hbar}}, \end{aligned} \quad (\text{A11})$$

where the pre-exponential factors are the Jacobians associated with the transformation of the path integral from the time-space to the frequency-space.⁴¹ ($q_{k,\ell}^R, q_{k,\ell}^I$) denote respectively the real and imaginary part of $q_{k,\ell}$. The integral Eq. (A11) has the general Gaussian form and its evaluation is straightforward. After some algebra, the relevant exponential term is

$$\Delta \mathcal{Z} \sim \exp \left\{ \frac{\beta\hbar}{8E_C} \sum_{\ell=0}^{\infty} Y(\omega_\ell) \frac{(\omega_\ell^2 + \omega_p^2)}{1 + \delta_{\ell,0}} |\theta_\ell|^2 \right\}, \quad (\text{A12})$$

with

$$Y(\omega_\ell) = \frac{1}{N-1} \sum_{k=1}^{k_{max}} \frac{\sin^2 \left(\frac{2\pi k}{N-1} \right)}{1 - \cos \left(\frac{2\pi k}{N-1} \right) + \frac{\pi^2}{2\lambda^2} \left(\frac{\omega_\ell^2}{\omega_\ell^2 + \omega_p^2} \right)}. \quad (\text{A13})$$

By adding the exponential term of Eqs. (A12),(A13) to the Lagrangian \mathcal{L}_1 Eq. (29) and going back to the time representation, we obtain the result shown in Eqs. (37), (38), and (39).

Appendix B: Instanton solution in periodic parabolic potential

Referring to the action Eq. (53), we set $\hbar\omega_J = 4V_J e^2 / (C^* + C_0/2)$ as a short-hand notation. The most general path can be always expressed as

$$\theta(\tau) = \theta(-\beta/2) + \int_{-\beta/2}^{\tau} d\tau' \dot{\theta}(\tau'). \quad (\text{B1})$$

For the asymptotic instanton-like solution, we require the following boundary conditions at the end-points $\theta_i = \theta(-\beta/2)$ and $\theta_f = \theta(\beta/2)$

$$\lim_{\beta \rightarrow +\infty} \theta_i = 0, \quad \lim_{\beta \rightarrow +\infty} \theta_f = \Delta\theta^*. \quad (\text{B2})$$

It is useful to use the Fourier components of the velocity as free variables

$$\dot{\theta}(\tau) = \sum_{\ell=-\infty}^{+\infty} \dot{\theta}_\ell e^{i\omega_\ell \tau}, \quad \dot{\theta}_\ell = \frac{1}{\beta} \int_{-\beta/2}^{\beta/2} d\tau \dot{\theta}(\tau) e^{-i\omega_\ell \tau}. \quad (\text{B3})$$

By assuming that the total energy is conserved, we impose that the initial velocity is equal to the final one: $\dot{\theta}(-\beta/2) = \dot{\theta}(\beta/2)$. More specifically, due to the symmetry of the potential, we can assume that the velocity is an even function of the time $\dot{\theta}(\tau) = \dot{\theta}_0 + \sum_{\ell=1}^{+\infty} 2 \cos(\omega_\ell \tau) \dot{\theta}_\ell$, with $\dot{\theta}_\ell$ are real numbers. By definition, the average velocity is $\dot{\theta}_0 = (\theta_f - \theta_i)/\beta$. In terms of the variables $\{\dot{\theta}_\ell\}$, the path Eq. (B1) reads

$$\theta(\tau) = \theta_i + \dot{\theta}_0 (\tau + \beta/2) + \sum_{\ell \neq 0} \left(\frac{e^{i\omega_\ell \tau} - e^{-i\omega_\ell \frac{\beta}{2}}}{i\omega_\ell} \right) \dot{\theta}_\ell. \quad (\text{B4})$$

We recall the definition of the kernel $G(\tau)$ in the action Eq. (53) in the Fourier space

$$G(\tau) = \frac{1}{\beta} \sum_{\ell \neq 0} G_\ell e^{i\omega_\ell \tau}, \quad \text{with } G_{-\ell} = G_\ell^*. \quad (\text{B5})$$

Using the expressions Eqs. (B3),(B4),(B5) in the action Eq. (53) and taking into account the symmetry respect to the time, the time integration is straightforward. The

general action is thus expressed in term of the variables $\{\dot{\theta}_\ell\}$

$$\begin{aligned} \frac{1}{\beta} S_p(\{\theta_\ell\}) &= \frac{V_J}{2\omega_J^2} \dot{\theta}_0^2 + \sum_{\ell=1}^{+\infty} \left(\frac{V_J}{\omega_J^2} + \frac{V_J}{\omega_\ell^2} + \frac{G_\ell}{\omega_\ell^2} \right) \dot{\theta}_\ell^2 \\ &- \sum_{\ell=1}^{+\infty} \frac{4V_J}{\beta\omega_\ell^2} \left[\theta_i (1 - (-1)^\ell) + \frac{\beta\dot{\theta}_0}{2} \right] \dot{\theta}_\ell \\ &+ \frac{V_J}{2} \left[\theta_i^2 + \frac{\beta\dot{\theta}_0}{2} \theta_i + \frac{(\beta\dot{\theta}_0)^2}{12} \right]. \end{aligned} \quad (\text{B6})$$

Then, by the condition of minimization $\partial S_p / \partial \dot{\theta}_\ell = 0$, we find the classical solution $\dot{\theta}_\ell^{(cl)}$

$$\dot{\theta}_\ell^{(cl)} = \frac{2\omega_J^2/\beta}{\omega_\ell^2 + \omega_J^2 + \frac{G_\ell}{V_J}\omega_J^2} \left[[1 - (-1)^\ell] \theta_i + \frac{\beta\dot{\theta}_0}{2} \right]. \quad (\text{B7})$$

We insert the solution Eq. (B7) into the action Eq. (B6) to obtain the value of the action at the minimum

$$\frac{S_p^{(cl)}}{\hbar} = \frac{\beta V_J \dot{\theta}_0^2}{2\hbar\omega_J^2} + \frac{4V_J}{\hbar\beta} \sum_{\ell=1}^{+\infty} \frac{\left[[1 - (-1)^\ell] \theta_i + \frac{\beta\dot{\theta}_0}{2} \right]^2}{\omega_\ell^2 + \frac{\omega_J^2}{1 + \omega_J^2 G_\ell / (\omega_\ell^2 V_J)}}. \quad (\text{B8})$$

Finally, we take the limit $\beta \rightarrow \infty$. We use the boundary conditions Eq. (B2) and the fact that the average velocity $\dot{\theta}_0$ scales as $(\theta_f - \theta_i)/\beta \simeq \Delta\theta^*/\beta$. After that, the resulting series with respect to Matsubara frequencies $\ell = 1, \dots, \infty$ converges to an integral $\omega_\ell = \omega$ and the resulting action coincides with Eq. (54) of the main text by recalling $\hbar\omega_J = 4V_J e^2 / (C^* + C_0/2)$ and Eq. (48) for $\Delta\theta^*$.

Appendix C: Long JJ ring with ground capacitance

In this Appendix we discuss some general features and some analytic limits of the effective action obtained within the parabolic approximation Eq. (54). To simplify the notation we set $V_J = E_J$ as the results are qualitatively the same for two different coefficients. We focus on the *long circumferences limit* of the rings defined by the condition that we can neglect the corrections of order $(1/N)$ in E_C^* , E_J^* and $\Delta\theta^*$ as well as $N \gg \max(\lambda, 1)$. In this regime, we replace the sum with respect to the modes k in $G(\omega_\ell) \equiv G(\omega)$ Eq. (39) with an integral and we obtain

$$G(\omega) = \frac{(\hbar\omega)^2}{16e^2} C_0 \left(F(\omega) \sqrt{1 + \frac{4C}{C_0}} - 1 \right), \quad (\text{C1})$$

where we set

$$F(\omega) = \sqrt{1 + \frac{\omega_{max}^2}{\omega^2}} \left[1 - \frac{2}{\pi} \arctan \left(\frac{\omega_{min}}{\omega} \sqrt{1 + \frac{\omega_{max}^2}{\omega^2}} \right) \right], \quad (\text{C2})$$

where $\omega_{max}, \omega_{min}$ are defined in Eqs. (22),(25). Note that we can not neglect the N -dependence in the function $F(\omega)$, Eq. (C2), as it is strongly dependent on the minimum cut-off frequency ω_{min} . Using the Eqs. (C1),(C2), we can express the action on the classical instanton path Eq. (54) as

$$\frac{S_p^{(cl)}}{\hbar} = 2\pi \frac{E_J}{\hbar} \int_0^\infty d\omega \frac{1}{\omega^2 + \frac{\omega_{max}^2}{1 + 2F(\omega)/(1 + 4C/C_0)^{1/2}}}. \quad (\text{C3})$$

The two frequencies $\omega_{max}, \omega_{min}$ define three ranges for the integral on the frequency ω . They are: i) $\omega_{max} \ll \omega$, ii) $\omega_{min} \ll \omega \ll \omega_{max}$, and iii) $\omega \ll \omega_{min}$. In these range the function $F(\omega)$ can be approximated as: i) $F(\omega) \simeq 1$, ii) $F(\omega) \simeq \omega_{max}/\omega$, and iii) $F(\omega) \simeq (N/\pi)/(1 + 4C/C_0)^{1/2}$, to leading order in $1/N$. Cutting the integral Eq. (C3) in three parts, we use the three approximated expression for the function $F(\omega)$ to evaluate the integration

$$\int_0^{+\infty} d\omega \dots = \int_{\omega_{max}}^{+\infty} d\omega \dots + \int_{\omega_{min}}^{\omega_{max}} d\omega \dots + \int_0^{\omega_{min}} d\omega \dots \quad (\text{C4})$$

The first integral i) in the high-frequency range as well as the third integral iii) in the low-frequency range gives a result independent of the ring's size N . On the other hand, for the second integral ii) in the intermediate frequency range we find the important result

$$\begin{aligned} \frac{S_p^{(cl)}}{\hbar} &\sim 2\pi \frac{E_J}{\hbar} \int_{\omega_{min}}^{\omega_{max}} d\omega \frac{1}{\omega^2 + \omega \omega_{max} (1 + 4C/C_0)^{1/2}} \\ &\sim \pi \sqrt{\frac{E_J}{8E_0}} \log \left(\frac{N}{\lambda} \right) + \dots \end{aligned} \quad (\text{C5})$$

As we have reported numerically, we have a logarithmic dependence on N of the classical action yielding to a power-law dependence of the QPS amplitude ν . This leads to a superconductor/insulator phase transition when the limit $N = \infty$ is taken.

Finally, we observe that the function $F(\omega)$ Eq. (C2) saturates to a constant for $\omega \ll \omega_{min}$. This low-frequency cut-off is important because it makes that the total integral convergent. As we have explained in the text, below this threshold $\omega \ll \omega_{min}$, the winding junction feels the discreteness of the spectrum of the environment with which it can exchange energy. That corresponds to say that there is no real dissipation at low frequency and an instanton solution conserving the initial energy still exists.

- ¹ L. B. Ioffe, M. V. Feigel'man, A. Ioselevich, D. Ivanov, M. Troyer, and G. Blatter, *Nature* **415**, 503 (2002).
- ² L. B. Ioffe and M. V. Feigel'man, *Phys. Rev. B* **66**, 224503 (2002).
- ³ B. Douçot and J. Vidal, *Phys. Rev. Lett.* **88**, 227005 (2002).
- ⁴ B. Douçot, M. V. Feigel'man, and L. B. Ioffe, *Phys. Rev. Lett.* **90**, 107003 (2003).
- ⁵ B. Douçot, M. V. Feigel'man, L. B. Ioffe, and A. S. Ioselevich, *Phys. Rev. B* **71**, 024505 (2005).
- ⁶ S. Gladchenko, D. Olaya, E. Dupont-Ferrier, B. Douçot, L. B. Ioffe, and M. E. Gershenson, *Nat. Physics* **5**, 48 (2009).
- ⁷ M. A. Castellanos-Beltrana and K. W. Lehnert, *Applied Physics Letters* **91**, 083509 (2007).
- ⁸ M. A. Castellanos-Beltrana, K. D. Irwin, G. C. Hilton, and L. R. Vale, *Nat. Physics* **4**, 928 (2008).
- ⁹ W. Guichard and F. W. J. Hekking, *Phys. Rev. B* **81**, 064508 (2010).
- ¹⁰ J. Flowers, *Science* **306**, 1324 (2004).
- ¹¹ V. E. Manucharyan, J. Koch, L. I. Glazman, and M. H. Devoret, *Science* **326**, 113 (2009).
- ¹² C. Hutter, E. A. Tholén, K. Stannigel, J. Lidmar, and D. B. Haviland, *Phys. Rev. B* **83**, 014511 (2011).
- ¹³ R. M. Bradley and S. Doniach, *Phys. Rev. B* **30**, 1138 (1984).
- ¹⁴ S. E. Korshunov, *Sov. Phys. JETP* **63**, 1242 (1986).
- ¹⁵ S. E. Korshunov, *Sov. Phys. JETP* **68**, 609 (1989).
- ¹⁶ R. Fazio and H. van der Zant, *Phys. Rep.* **355**, 235 (2001).
- ¹⁷ S. Sarkar, *Phys. Rev. B* **75**, 014528 (2007).
- ¹⁸ S. Sarkar, *Eur. Phys. J. B* **67**, 559 (2009).
- ¹⁹ E. Chow, P. Delsing, and D. B. Haviland, *Phys. Rev. Lett.* **81**, 204 (1998).
- ²⁰ D. B. Haviland, K. Andersson, and P. Ågren, *Jour. of Low Temp. Physics* **118**, 733 (2000).
- ²¹ W. Kuo and C. D. Chen, *Phys. Rev. Lett.* **87**, 186804 (2001).
- ²² H. Miyazaki, Y. Takahide, A. Kanda, and Y. Ootuka, *Phys. Rev. Lett.* **89**, 197001 (2002).
- ²³ Y. Takahide, H. Miyazaki, and Y. Ootuka, *Phys. Rev. B* **73**, 224503 (2006).
- ²⁴ K. A. Matveev, A. I. Larkin, and L. I. Glazman, *Phys. Rev. Lett.* **89**, 096802 (2002).
- ²⁵ I. M. Pop, I. Protopopov, F. Lecocq, Z. Peng, B. Pannetier, O. Buisson, and W. Guichard, *Nat. Physics* **6**, 589 (2010).
- ²⁶ T. P. Orlando, J. E. Mooij, L. Tian, C. H. van der Wal, L. S. Levitov, S. Lyod, J. J. Mazo, *Phys. Rev. B* **60**, 15398 (1999).
- ²⁷ K. K. Likharev and A. B. Zorin, *J. Low Temp. Phys.* **59**, 347 (1985).
- ²⁸ G. Catelani, R. J. Schoelkopf, M. H. Devoret, and L. I. Glazman, *Phys. Rev. B* **84**, 064517 (2011).
- ²⁹ Note that Eq. (1) corresponds to $\bar{\epsilon}/2$ in Eq. 100 of Ref.28.
- ³⁰ N. A. Masluk, I. M. Pop, A. Kamal, Z. K. Mineev, and M. H. Devoret, *Phys. Rev. Lett.* **109**, 137002 (2012).
- ³¹ A. O. Caldeira and A. J. Leggett, *Phys. Rev. Lett.* **46**, 211 (1981).
- ³² A. Schmid, *Phys. Rev. Lett.* **51**, 1506 (1983).
- ³³ Note that the model discussed here is different from the one introduced by Z. Hermon, E. Ben-Jacob, and G. Schön, *Phys. Rev. B* **54**, 1234 (1996) in which the kinetic inductance of the superconducting grains was assumed to be much larger than the Josephson inductance. Here we consider the experimentally more relevant opposite regime where the Josephson inductance dominates (see also Ref. 34).
- ³⁴ F. W. J. Hekking and L. I. Glazman, *Phys. Rev. B* **55**, 6551 (1997).
- ³⁵ M. Tinkham, *Introduction to Superconductivity* (McGraw-Hill int. eds., Singapore 1996, 2nd edition).
- ³⁶ I. M. Pop, B. Douçot, L. Ioffe, I. Protopopov, F. Lecocq, I. Matei, O. Buisson, and W. Guichard, *Phys. Rev. B* **85**, 094503 (2012).
- ³⁷ The detailed comparison of our result with Eq. (8) of Ref. 15 requires the substitution $E_J \rightarrow \hbar V$ and $\hbar^2 C/(4e^2) \rightarrow M, \hbar^2 C_0/(4e^2) \rightarrow m$.
- ³⁸ G. Schön and A.D. Zaikin, *Phys. Rep.* **198**, 237 (1990).
- ³⁹ G. Rastelli, *Phys. Rev. A* **86**, 012106 (2012).
- ⁴⁰ P. R. Johnson et al., *Phys. Rev. Letts.* **94**, 187004 (2005); J. M. Schmidt, A. N. Cleland, and J. Clarke, *Phys. Rev. B* **43**, 229 (1991).
- ⁴¹ H. Kleinert, *Path Integral in Quantum Mechanics, Statistics and Polymer Physics*. (World Scientific, Singapore 1995, 2nd edition).
- ⁴² J. Villain, *J. Phys. (Paris)* **36**, 581 (1975).
- ⁴³ Note that for $G(\omega) = 0$ ($C_0 = 0$), the integral converges to the factor $\pi/2$ and we obtain $S_{par}/\hbar = 8(\Delta\theta^*/(2\pi))^2 \sqrt{E_J^*/E_C^*}$. Actually, this result is slightly different from the one obtained with the cosine potential Eq. (49). In the latter case, the classical action depends linearly on $\Delta\theta^*/(2\pi) = 1 - 1/N$. At finite length, finite size corrections in $1/N$ carry a different numerical prefactor.
- ⁴⁴ A. J. Leggett, S. Chakravarty, A. T. Dorsey, M. P. A. Fisher, A. Garg, and W. Zwerger, *Rev. Mod. Phys.* **59**, 1 (1987).
- ⁴⁵ Notice that, when we consider the regime $C_0 > 0$ and $N \gg \lambda$, the condition of validity $N < N^*$ also implies an upper bound to the parameter q defined in Eq. (14).